CARBON CAPTURE POTENTIAL OF LOCAL SLAG WASTE STREAMS THROUGH ASSESSING THE CARBON CAPTURE CAPACITY OF ELECTRIC ARC FURNACE (EAF) SLAG

SIOW YEE HENG

UNIVERSITI TUNKU ABDUL RAHMAN

CARBON CAPTURE POTENTIAL OF LOCAL SLAG WASTE STREAMS THROUGH ASSESSING THE CARBON CAPTURE CAPACITY OF ELECTRIC ARC FURNACE (EAF) SLAG

SIOW YEE HENG

A project report submitted in partial fulfilment of the requirements for the award of Bachelor of Civil Engineering with Honours

Lee Kong Chian Faculty of Engineering and Science
Universiti Tunku Abdul Rahman

April 2024

DECLARATION

I hereby declare that this project report is based on my original work except for citations and quotations which have been duly acknowledged. I also declare that it has not been previously and concurrently submitted for any other degree or award at UTAR or other institutions.

Signature   :

Name   : Siow Yee Heng

ID No.   : 1902383

Date   : 22/04/2024

APPROVAL FOR SUBMISSION

I certify that this project report entitled **"CARBON CAPTURE POTENTIAL OF LOCAL SLAG WASTE STREAMS THROUGH ASSESSING THE CARBON CAPTURE CAPACITY OF ELECTRIC ARC FURNACE (EAF) SLAG"** was prepared by **SIOW YEE HENG** has met the required standard for submission in partial fulfilment of the requirements for the award of Bachelor of Civil Engineering with Honours at Universiti Tunku Abdul Rahman.

Approved by,

Signature   :

Supervisor   :   Ir. Ts. Dr. Lee Foo Wei

Date   :   29/04/2024

Signature   :

Co-Supervisor   :

Date   :

The copyright of this report belongs to the author under the terms of the copyright Act 1987 as qualified by Intellectual Property Policy of Universiti Tunku Abdul Rahman. Due acknowledgement shall always be made of the use of any material contained in, or derived from, this report.

ABSTRACT

Nowadays, a growing concern is about carbon dioxide emissions that are reaching unprecedented levels, which thus require urgent measures to appease them. As time goes on and industries begin enlarging and producing steel slag as a waste product, the problem of disposal is becoming urgent. However, amidst this challenge lies an opportunity because capturing carbon dioxide by utilising slag waste also tackles ecological problems and assists in the fight against climate change. This innovative approach not only mitigates the burden of carbon emissions, but industrial waste is also transformed into a valuable resource that contributes to sustainability and resilience in the wake of an accelerating environmental crisis. In this study, the carbon capture potential of local slag waste streams is analysed by assessing the carbon capture capacity of electric arc furnace (EAF) slag through concrete production. Ten sets of concrete were prepared: R1 (2.36 mm - 0.8 mm), R2 (4.75 mm - 2.36 mm), and R3 (7 mm - 4.75 mm) at replacement percentages of 15 %, 30 %, and 45 %. The control set was prepared with one set as normal concrete while the other nine sets of concrete were added with EAF slag as EAF slag concrete. After conducting and going through a series of tests such as compression tests, X-ray diffraction (XRD), scanning electron microscopy (SEM), and energy-dispersive X-ray spectroscopy (EDS), the results are analysed and discussed. The EDS study suggests the optimum particle size range for carbon capture efficiency is R2. These particles have a higher concentration of carbon (2.61%), silicon, and calcium (82.2 %), and a more uniform elemental composition. Carbon capture capacity was also evaluated by the XRD method. The greatest result, 18.41 %, was obtained as R2 at 45 % replacement. The compression tests resulted in the addition of EAF slag, which significantly enhanced the compressive strength of concrete specimens. R3 at the 45 % replacement level achieved the highest compressive strength as 879.90 MPa and showed higher compressive strength than normal concrete overall. This outcome, which highlights environmental regulations and the new era of construction, conforms to the research title, goals, and objectives. The paper assists the construction industry in building up a more

sustainable one by utilising local slag waste streams to increase or replace the carbon capture capability in concrete production.

TABLE OF CONTENTS

LIST OF TABLES

LIST OF FIGURES

LIST OF SYMBOLS / ABBREVIATIONS

AOD	argon oxygen decarburizing
BOF	basic oxygen furnace
CCU	carbon capture and utilisation
CCS	carbon capture and storage
CFD	computational fluid dynamics
CO_2	carbon dioxide
DTG	first-differential thermogravimetric
EAF	electric arc furnace
EDS	energy-dispersive X-ray spectroscopy
EPMA	electron probe microanalysis
IEA	International Energy Agency
IPCC	Intergovernmental Panel on Climate Change
LF	ladle refining
NA	natural aggregate
NETL	National Energy Technology Laboratory
OPC	ordinary Portland cement
SS	steelmaking slag
SEM	scanning electron microscopy
TGA	thermogravimetric analysis
XRD	X-ray diffraction

LIST OF APPENDICES

CHAPTER 1

INTRODUCTION

1.1   General Introduction

Reducing carbon dioxide (CO_2) emissions is as urgent as ever in today's global battle against climate change. Unconventional carbon capture methods have come under the spotlight as industries seek innovative solutions to reduce their carbon footprint. Among these methods, one of the hidden gems is found in local waste streams: Electric Arc Furnace (EAF) slag. A by-product of steel production, EAF slag has a remarkable capacity for carbon capture, offering a promising avenue for both waste management and climate change mitigation. This report highlights the importance of EAF slag in the broader landscape of carbon sequestration technologies and explores the carbon capture potential of EAF slag sourced from local waste streams.

Carbon dioxide (CO_2) is a chemical compound formed by a molecule consisting of one carbon atom bonded to two oxygen atoms. CO_2 usually exists in gaseous form at room temperature and has many sources. Both natural and human sources can produce CO2. The decay of flora and fauna, the respiration of living organisms, open burning, and the burning of fossil fuels are good examples of sources of CO_2. CO_2 is also a greenhouse gas that causes global warming and climate change. According to Grace (2013), the carbon cycle is a natural cycle that links the biosphere, atmosphere, geosphere, and hydrosphere. The carbon cycle describes the activities of carbon from the atmosphere and between the major components of the Earth system. It is important to maintain the balance of the carbon cycle. Although the existence of the carbon cycle helps maintain the carbon concentration naturally, the balance of the carbon cycle is still being disturbed by human activities, resulting in the increasing concentration of CO_2. It is also important to note that the steel industry contributes around 8 % of total global carbon dioxide emissions, a figure that is expected to increase as crude steel production grows. In 2021, for example, the global production of crude steel will reach 1.952 billion tonnes. It is estimated that one tonne of steel produces approximately 2 tonnes of carbon dioxide emissions and 600 kg of slag. As a result, the annual

global production of steelmaking slag has exceeded 250 million tonnes. Therefore, solutions must be found to solve the problem.

1.2 Importance of the Study

The study of the carbon capture potential of local slag waste streams, in particular by accessing the carbon capture capacity of electric arc furnace (EAF) slag, is of significant importance and offers global benefits. Carbon capture, which includes concepts such as Carbon Capture and Storage (CCS) and Carbon Capture and Utilisation (CCU), plays a key role in addressing the challenges of CO_2 emissions and production. The following examples illustrate how the use of EAF slag in carbon capture initiatives is helping to address the global problem of CO_2 emissions.

Utilisation of EAF slag helps in mitigating climate change. The steel industry is one of the major contributors to CO_2 emissions, with annual production accounting for a significant proportion of global emissions. By utilising the carbon capture capacity of EAF slag, the impact of these emissions can be mitigated and contribute to the global effort to combat climate change.

Next, EAF slag has CO_2 reduction potential. As a by-product of steelmaking, EAF slag offers a promising way to capture and store CO_2 emissions. By incorporating EAF slag into carbon capture technologies, the amounts of CO_2 from the atmosphere can be removed significantly, thereby reducing greenhouse gas concentrations and mitigating climate change.

Moreover, utilisation of EAF slag in carbon capture is a step towards a low carbon economy. Harnessing the carbon capture capacity of EAF slag facilitates the transition to a low carbon economy. By using EAF slag in carbon capture processes, the carbon intensity reduced associated with steel production, thereby promoting sustainable practices in the construction industry, and contributing to a greener economy.

Lastly, utilisation of EAF slag in carbon capture is an advanced resource management. The inclusion of EAF slag in carbon capture initiatives is consistent with the principles of advanced resource management. Using waste materials such as EAF slag minimises reliance on finite resources, reducing the environmental impact of construction activities. In addition, the

by-products of carbon capture processes, such as carbonate minerals, can be used in various applications, further enhancing resource efficiency and sustainability.

In conclusion, the construction industry's investigation and implementation of carbon capture concepts, such as the use of EAF slag for carbon capture, has immense potential to combat climate change, reduce CO_2 emissions, and promote a greener and more sustainable future. By harnessing the carbon capture capacity of EAF slag, we can use local waste streams to address global environmental challenges and support international efforts towards a more sustainable world.

1.3   Problem Statement

The problem statement in this report is the issues raised by the heavy CO_2 production and emissions due to the construction field. Although the construction sector contributes significantly to the growth of the world economy by creating structures, infrastructure, facilities, and other necessary infrastructure to support all human societies, this sector also contributes significantly to carbon dioxide (CO_2) emissions. The contribution mostly comes from steel and cement production. This is because cement and steel are essential building materials, and a lot of energy is consumed and a lot of greenhouse emissions, especially CO_2 are produced during their manufacturing processes. Hence, the current issue is the excessive CO_2 emissions produced due to the operation of steel and cement factories in the construction industry. These emissions are of a sizeable magnitude, contributing to climate change and creating environmental problems. It is crucial to address and reduce the impact of CO_2 emissions from cement and steel production due to the increasing demand for construction materials and the rapid development of infrastructure.

1.4   Aim and Objectives

This study aims to assess the effectiveness of EAF slag in carbon capture capacity and explore the performance of EAF slag concrete with conventional concrete. The objectives of this study are:

(i)   To determine the optimum particle size range of EAF slag for carbon capture.

(ii)   To evaluate the carbon capture capacity of EAF slag.

(iii) To compare the compressive strength of EAF slag concrete and conventional concrete.

1.5   Scope and Limitation of the Study

The scope of this study is to determine the carbon capture potential of local slag waste stream by assessing the carbon capture capacity of EAF steel slag. The study explores various mineralization methods available worldwide, such as in situ carbonation, ex-situ carbonation, direct carbonation, indirect carbonation, and others. However, it is important to note that this study has limitations, primarily restricted to the scarcity of sample types and sources. This report specifically focuses on EAF slag, a type of steel slag, while acknowledging the presence of various other types of steel slag within the local waste stream in Malaysia. Other than that, the samples in this report originate from only one source in Malaysia, which is Penang. This scarcity of sample sources may affect the accuracy of the results since there is an insufficiency of comparative data from other sources. Additionally, the study utilises fixed analysis methods, including X-ray diffraction (XFD), scanning electron microscopy (SEM), and energy-dispersive X-ray spectroscopy (EDS). Other techniques were not considered due to the unavailability of experimental equipment, materials, and methodologies.

1.6   Contribution of the Study

The carbon capture potential of the local waste stream through accessing the carbon capture capacity of EAF slag is investigated in this study. This study results in several valuable contributions, including waste reduction, carbon capture, and cost savings.

The reuse of EAF slag, a by-product of steel production, as a medium for carbon capture effectively minimizes waste generation while addressing the environmental impacts associated with waste disposal. This approach reduces the pressure on landfill sites and conserves valuable land resources. Besides, the utilisation of EAF slag promotes the circular economy as the inclusion of EAF slag in carbon capture initiatives is in line with the principles of the circular economy. The circular economy seeks to minimise waste and maximise resource use, rather than following a linear model of production, consumption, and disposal. By transforming EAF slag from waste into a valuable resource for capturing carbon, the industry contributes to the circular economy paradigm and promotes a more resilient and sustainable economic model. In addition, utilising the carbon capture capacity of EAF slag provides a practical and efficient means of capturing and storing CO_2 emissions, contributing to global efforts to combat climate change by reducing the impact of greenhouse gas emissions. As carbon emissions become an increasingly pressing global concern, nations around the world are actively seeking to reduce their carbon footprint through a variety of means. Countries can reduce their carbon footprint and industries can proactively meet regulatory requirements and demonstrate environmental compliance by adopting carbon capture technologies using EAF slag. In addition, the use of EAF slag for carbon capture offers potential cost savings compared to traditional methods. EAF slag as a by-product of the steel-making process is often readily available and can be sourced at a lower cost than specialised carbon capture materials, industries can realise significant savings while reducing the logistical challenges associated with material transport and processing.

In summary, industries can address environmental concerns and pave the way for more sustainable and cost-effective industrial practices by harnessing the carbon capture potential of EAF slag from local waste streams.

1.7 Outline of the Report

The structure of this report is divided into five chapters to give a thorough review of the carbon capture potential of the local waste stream by accessing the carbon capture capacity of EAF slag.

Chapter 1 provides a concise overview of the general introduction, the importance of the study, and problem statements about the title of the final year project. In this chapter, the aim and objectives, scope and limitation of the study as well as the report structure are also stated clearly.

Chapter 2 present literature review to gain more understanding of the study. This chapter is further divided into several headings such as general introduction, type of mineralization techniques, and type of analysis methods to have a more detailed study of the title.

Chapter 3 illustrates the methodology of the study. Flowchart, raw materials preparation, experiment procedure, and analysis process are stated in this methodology section.

Chapter 4 presents the results and discussions in this chapter. Experiment results are shown in graphs and tables to give a clearer picture and be more systematic. Discussion and comparison of the results are another major section in this chapter which eventually helps in concluding the results.

Chapter 5 summarizes and concludes the results of the entire report and offers recommendations, if necessary, based on the findings.

CHAPTER 2

LITERATURE REVIEW

2.1   Introduction

A literature review is a process to get useful information and knowledge of relevant topics by conducting surveys on scholarly articles, journals, reference books, or other research papers. In this report, the literature review is focused on the carbon capture potential of local waste streams by accessing the carbon capacity of EAF slag. The findings of the literature review are based on a few keywords. For example, carbon capture, steel slags, EAF slag, evaluated performance, CO_2 conversion, carbonate minerals, and analysis methods. By referring to the literature review that was conducted, an overview of the study is presented in this chapter. The literature review helps in giving a clearer picture and understanding to the readers and researchers. Moreover, the literature review also guides the task neatly and outlines the content for the following chapters. This will be clearly shown in Chapter 3 Methodology, Chapter 4 Result and Discussion, and the last chapter of this report the Conclusion, which concludes that the study can achieve the aim and objectives mentioned in the first chapter as well.

2.2   Carbon Capture and Storage

Carbon capture and storage (CCS) is a technique used to reduce carbon dioxide (CO_2) emissions from power plants and industrial activities. It involves removing CO_2 from large-scale emission sources, for example, factories and power plants. Then, the CO_2 is stored underground in geological formations to prevent it from being emitted into the atmosphere. Some of the examples of the methods used to capture CO_2 are post-combustion capture, pre-combustion capture, and oxy-fuel combustion (Rahmanihanzaki and Hemmati, 2022).

CCS consists of three steps which are carbon capture, transport, and storage. First, CO_2 is captured through some methods from various sources before it is released into the atmosphere. Secondly, the CO_2 gas is compressed into the form of liquid and then transported to the storage site after the capture

step. The last step of CCS is storing the acquired CO_2 in safe geological formations, like deep rock formations underground or depleted oil and gas reservoirs. By injecting CO_2 into these geological formations, the CO_2 eventually becomes trapped and mineralizes, preventing it from escaping into the atmosphere.

CCS is one of the effective methods to reduce CO_2 emissions and prevent climate change. The burning of fossil fuels is the main cause of CO_2 emissions today as it makes up 80–85 % of all energy sources used in the world. Fossil fuel consumption is estimated to continue for decades due to the factor of abundance, low cost, and gradual shift to renewable energy. Hence, it will cause a continual rise in atmospheric CO_2 levels and global warming. Since the first step of CCS is capturing CO_2 released from sources, CCS solves the problem of 60 % of CO_2 emissions entering the atmosphere by preventing CO_2 from entering the atmosphere (Rahmanihanzaki and Hemmati, 2022).

According to Rahmanihanzaki and Hemmati (2022), CCS shows satisfactory results and efficiency in reducing CO_2 and greenhouse gas emissions by 72 % to 90 % and 65 % to 79 % respectively. With these results, CCS leads to a substantial reduction in CO_2 and greenhouse gas emissions. However, the drawbacks of CCS which are high capital costs of constructing facilities for carbon capture, unprofitability, and global financial issues have caused the implementation of CCS constrained in several countries like the United States and the United Kingdom.

2.3   Carbon Capture and Utilisation (CCU)

A new method called carbon capture and utilisation (CCU) has become an attractive alternative to replace carbon capture and storage (CCS). This is because CCUs do not have disadvantages like high capital costs, unprofitability, and long-term carbon storage issues as compared to CCS. CCU is more concerned with converting carbon dioxide into useful products, resulting in economic gains, and avoiding the drawbacks of CCS techniques. Generally, CCU aims to transform captured CO_2 into a variety of useful goods, making it economically appealing and independent of specific CO_2 storage places, which may be inadequate in some nations. Next, the presence of post-

storage monitoring which is less costly makes CCU more cost-effective, and it is another advantage that CCS could not offer.

The procedure of CCU always starts with the separation of CO_2 from exhaust gases produced by the combustion of fossil fuels. Then, it is purified to produce valuable products, for example, eco-friendly CO_2-based polymers or chemical substances like formic acid, salicylic acid, and urea. A technique called direct air capture technique is also applied in CCU to directly capture CO_2 from the atmosphere. Currently, the utilisation of CO_2 is now widely implemented in enhanced oil and gas recovery and hydraulic fracturing among other techniques. However, efforts should be made to increase the usage of CO_2 in business sectors while addressing economic issues and promoting innovation at the same time. For example, CCU can be applied in various sectors such as chemical, pharmaceutical, and polymer sectors, as well as in beverage production, food preservation, urea manufacturing, water treatment, and chemicals and polymer synthesis. CCU provides the opportunity to replace or supplement the existing raw materials. Despite these developments, the statistic shows that only 1% and below of the current atmospheric CO_2 is utilised and converted to useful products, emphasizing again the significance of taking into account economic and environmental issues for extending CCU application (Rahmanihanzaki and Hemmati, 2022).

2.4   Electric Arc Furnace (EAF) Slags

Steelmaking slag (SS) is a by-product of the metallurgical industry and includes a range of types such as Basic Oxygen Furnace (BOF) slag, Electric Arc Furnace (EAF) slag, Argon Oxygen Decarburizing (AOD) slag and Ladle Refining (LF) slag (None Akhil and Singh, 2023). Figure 2.1 illustrates the different processes involved in steelmaking.
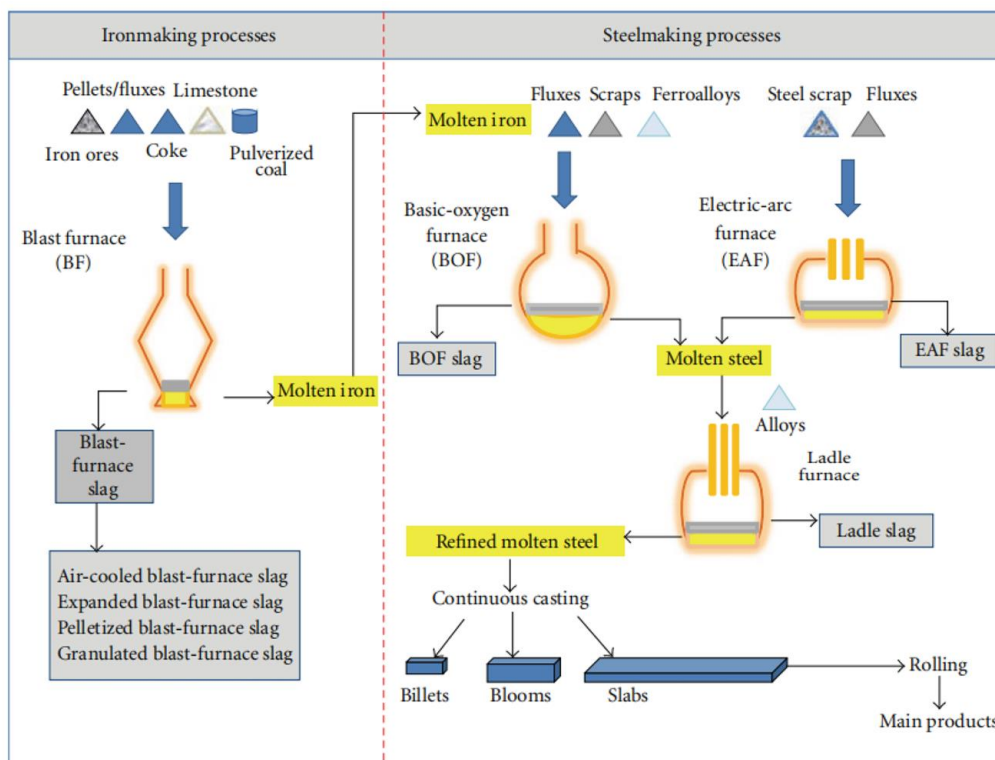
Figure 2.1: Processes of Steelmaking Slag Production (Zhang et al., 2023).

In today's integrated iron and steel plants, EAF technology is the predominant method of producing steel and iron. Electric arc furnace slag is produced from liquid steel in the range of 150 to 200 kg, as a by-product of liquid steel melting and primary acid refining (Sangita Meshram et al., 2023). EAF slag is a derivative of the iron and steel sector and is obtained from the electric arc furnace by the addition of flux at temperatures of 1700 °C, with steel scrap as the primary raw material (Rojas et al., 2023). During EAF operations, deslagging is a critical step aimed at removing impurities from the furnace. Undesirable materials in the molten bath undergo oxidation and transition to the slag phase. By tilting the furnace backwards and discharging the slag through the slag door, it is advantageous to efficiently remove phosphorus into the slag during the early stages of heating. This reduces the risk of phosphorus reversion, a phenomenon observed during the slag foaming process in which the injected carbon reduces the iron oxides to metallic iron and produces CO to facilitate the foaming of the slag (Singh, 2016). Failure to remove high phosphorus slag before this operation can result in phosphorus reversion. The slag contains various oxides and elements that are detrimental

to steel quality. A standard analysis of EAF slag, as shown in Table 2.1, highlights its main components.

Table 2.1: Electric Arc Furnace Slag (Singh, 2016).

Component	Source	Composition Range
CaO	Charged	40 – 60 %
SiO$_2$	Oxidation product	5 – 15 %
FeO	Oxidation Product	10 – 30 %
MgO	Charged as dolomite	3 – 8 %
CaF$_2$	Charged – slag fluidizer	-
MnO	Oxidation product	2 – 5 %
S	Absorbed from steel	-
P	Oxidation product	-

The basic characteristics of EAF slag include a relatively high mass resulting from its internal composition, typically between 3000 and 4000 kg per cubic metre.

2.5   Electric Arc Furnace (EAF) Slag in Construction

Industrial waste generation is increasing, particularly in developing countries, due to the large quantities produced and the limited land available to dispose of this waste. As Azevedo, A.R. et al. points out, the increase in municipal, industrial, and agricultural solid waste is a major environmental challenge. This underlines the urgent need for governments around the world to adopt more environmentally sustainable practices (Sangita Meshram et al., 2023). Many wastes have pozzolanic properties which, when combined with cement, improve the properties of the material. However, pozzolanic materials lack binding properties when used alone. It is therefore common for building materials such as bricks, concrete, and mortar to be made from wastes that would otherwise be discarded (Sangita Meshram et al., 2023). To reduce the impact of land pollution on the environment, industrial wastes such as cupola slag, steel furnace slag, ground granulated blast furnace slag, and electric arc furnace slag can be reused or recycled. EAF slag consists mainly of iron oxides, silicates, and calcium aluminates. It exhibits properties such as hardness, toughness, abrasion resistance, chemical stability, durability, and high density (Rojas et al., 2023). As a result, several researchers are proposing its use in the production of concrete as a trouble-free replacement for heavy

and fine natural aggregates (NA), depending on particle size requirements. EAF can also replace natural aggregates in concrete casting. Several studies have shown that certain by-products can be used as suitable replacements for NA in concrete production, or even as binders in cement, with the characteristics and properties contributed by NA (Rojas et al., 2023). It is expected that this approach will help to mitigate some of the environmental, economic, and social impacts associated with the use of NA. Thus, for the construction industry, and for concrete mixers, the use of electric arc furnace slag as a partial or total replacement for fine and coarse NA in the production of concrete is a promising alternative.

2.6   Concrete

Concrete is one of the most widely used materials in the world, second only to water in terms of consumption, which is around 12 billion tonnes per year. With a direct impact on infrastructure development and economic growth, its importance in the construction industry is undeniable. Concrete consists of approximately 10 - 20 % cement, 70 - 80 % natural aggregate (NA), and 5 – 10 % water by mass (Ren and Li, 2023). Concrete is a composite material that is bound together by a cement or binder, forming a matrix that encapsulates and adheres the aggregate particles (Chandini, 2017). These aggregates, typically sourced from natural rock such as crushed stone or gravel, are often extracted from riverbeds and rocks, resulting in the depletion of natural resources. The escalating demand for concrete has led to the over-exploitation of high-quality river sand and gravel, exacerbating environmental concerns. To mitigate these impacts, there is a growing emphasis on the use of iron and steel industry by-products in concrete production, providing a sustainable alternative and reducing reliance on virgin resources.

2.6.1   Ordinary Concrete

Ordinary concrete is the most common type of concrete used in construction. It is also known as normal strength concrete or conventional concrete. It typically consists of a mixture of cement, water, and aggregates such as sand, gravel, or crushed stone only. Ordinary concrete is sometimes used as the control set of research and experiments to compare the mechanical and

chemical properties with the other concrete sets. The mixed proportion design is important in deciding the strength of ordinary concrete. The proportions of these ingredients are carefully controlled to achieve the desired strength and durability for the intended application.

2.6.2   Electric Arc Furnace (EAF) Slag Concrete

Steel slag, a by-product of steel production, is gaining popularity as a replacement for traditional aggregates in concrete. This material is produced when molten steel is separated from impurities in furnaces. These impurities, including silica, phosphorus, carbon monoxide, manganese, and iron, solidify to form steel slag, which can be used in concrete as an aggregate or as a cementitious admixture (None Akhil and Singh, 2023). Incorporating steel slag into concrete offers environmental benefits by reducing the need for natural aggregates and by providing a sustainable outlet for industrial by-products. In addition, steel slag in concrete can improve certain properties such as strength and durability, making it an attractive option for construction projects.

There are several types of steel slag, the most common being electric arc furnace (EAF) slag, basic oxygen furnace (BOF) slag, and ladle furnace (LF) slag. EAF slag, for example, is produced during the manufacture of steel in electric arc furnaces. In this process, scrap steel is melted using high-powered electric arcs without the use of hot metal. Oxygen is blown into the furnace to refine the steel. As impurities rise to the surface, they form a layer of slag, which is then removed from the molten steel (Chandini, 2017). EAF slag is typically slightly darker and has a grey or grey-black colour. While the raw materials and production principles of EAF slag and BOF slag are similar, they may differ slightly in morphology and structure. However, both types of slag serve as valuable materials for various applications, including concrete production.

2.6.3   Compressive Strength

Compressive strength is of significant importance among the various strengths of concrete, as concrete is primarily designed to withstand compressive stress. It is considered a fundamental parameter in the quality assessment and design of concrete structures. Compressive strength plays a key role in the probabilistic reliability analysis of structures and is the basis for the determination of the characteristic value used in the concrete strength classification.

For reliable design and safety assessment of structural elements and concrete structures, it is crucial to understand the statistical properties of compressive strength, including mean value, dispersion, and probability distribution. This is usually done by casting cylinders or cubes from the same batch of concrete used in the construction and then curing them in the lab under controlled conditions. After a specified curing period, usually 28 days, these specimens are compression tested using a hydraulic machine until failure occurs. The maximum load just before failure is recorded as the compressive strength.

Various distribution functions such as normal, Weibull, and log-normal have been extensively studied as models to express the probability distribution of concrete compressive strength between different tests.

2.7   Type of Mineralisation Techniques

Mineralisation refers to the process of the transformation of an organic substance from its original state into inorganic components. Many fields hold the explanation of mineralisation. In this report, mineralisation that involves conversion of carbon dioxide into carbonate minerals is focussed. The mineralisation techniques play a crucial role in raw material preparation and the following experiments. The mineralisation techniques that aid in converting CO_2 into carbonate minerals such as in situ carbonation, ex-situ carbonation, natural carbonation, accelerated carbonation, carbonate precipitation using alkaline waste, and biological mineralisation are studied, reviewed, and presented in this chapter (Romanov et al., 2015).

2.7.1 Natural Carbonation

Natural carbonation is a process that can occur naturally, and normally this kind of natural carbonation is known as "weathering". The outcome of natural carbonation is the removal of CO_2 from the air through the neutralization of acidity using mineral alkalinity. In this natural weathering process, alkaline silicates found in nature will react with atmospheric CO_2. When atmospheric CO_2 dissolves in rainwater, it slightly increases the acidity of the rainwater due to the formation of a weak form of carbonic acid. The acidic rainwater then interacts with minerals in the earth's crust, especially with the calcium and magnesium silicates, causing them to dissolve and be carried by the rainwater to rivers and eventually into the ocean. In the ocean, these dissolved calcium and magnesium ions combine and are mineralised to form carbonate minerals (Pan, Chang, and Chiang, 2012).

The process of chemical weathering of natural mineral ores plays a critical role in the global geochemical carbon cycle. This natural cycle captures CO_2 in the form of mineral carbonates, which precipitate from the ocean over geological timeframes. However, the rate of natural carbonation is extremely slow due to the concentration of CO_2 in the atmosphere is relatively low, typically around 0.03 – 0.06 %. According to the investigation (Haug, Kleiv, and Munz, 2010), it is estimated that the rate of olivine weathering is $10^{-8.5}$ mol/(m²s) using the average ground temperature in Norway (6 °C) and a pH of 5.6, which corresponds to the acidity of rainwater. This indicates how slow the process occurs under these conditions.

2.7.2 Accelerated Mineral Carbonation

As mentioned before, carbonation can take place naturally. This natural carbonation is often referred to as "weathering," which gradually removes CO_2 from the air by using mineral alkalinity to neutralize acidity. Apart from natural carbonation, a new method known as accelerated carbonation has gained significant awareness through recent research and development. Alkaline materials react with high-purity CO_2 in the presence of moisture to increase the reaction rate, to just a few minutes or hours in accelerated carbonation (Pan, Chang, and Chiang, 2012). In Figure 2.3 below, the proposed mechanism for accelerated carbonation is depicted.
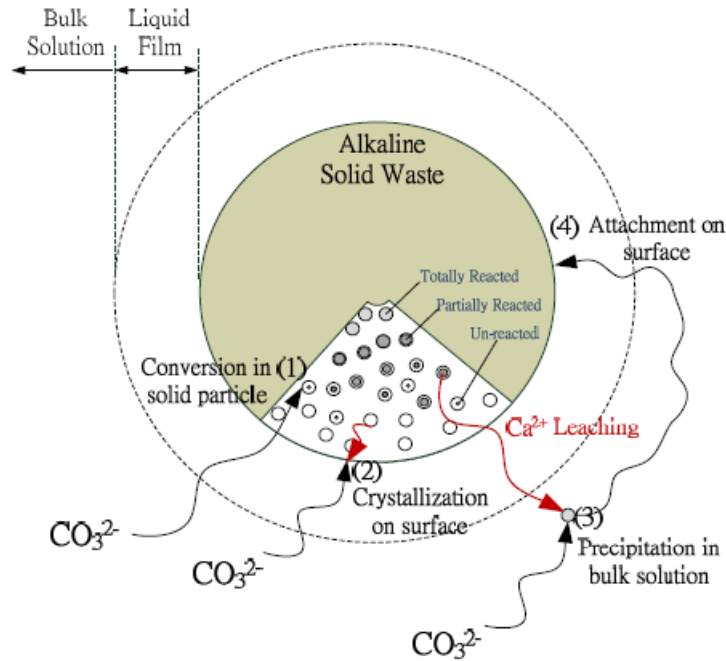
Figure 2.2: Mechanism of Accelerated Carbonation (Pan, Chang, and Chiang, 2012).

This diagram highlights that the carbonation process follows four different paths. According to Pan, Chang and Chiang (2012), the mechanisms that could influence the speed and extent of carbonation include:

(i)   transport-related processes involving the diffusion of CO_2 and Ca2+ ions to and from reaction sites.

(ii)   Effects related to the boundary layer (diffusion occurring across coatings formed on particles).

(iii) the dissolution of Ca (OH)2 at the particle's surface.

(iv)   blockage of pores.

(v)   the formation of precipitate coatings.

The fundamental chemical reactions of accelerated carbonation are presented in Equations (2.1) to (2.4):

$$Ca(OH)_{2(s)} + CO_{2(g)} \rightarrow CaCO_{3(s)} + H_2O_{(l)}, \Delta H = -\frac{113kj}{mol}CO_2 \quad (2.1)$$

$$Mg(OH)_{2(s)} + CO_{2(g)} \rightarrow MgCO_{3(s)} + H_2O_{(l)}, \Delta H = -\frac{81kj}{mol}CO_2 \quad (2.2)$$

$$CaO_{(s)} + CO_{2(g)} \rightarrow CaCO_{3(s)}, \Delta H = -\frac{178kj}{mol} CO_2 \qquad (2.3)$$

$$MgO_{(s)} + CO_{2(g)} \rightarrow MgCO_{3(s)}, \Delta H = -\frac{118kj}{mol} CO_2 \qquad (2.4)$$
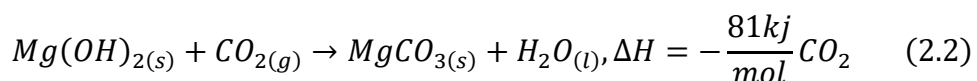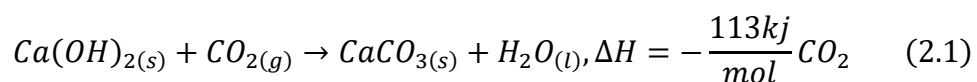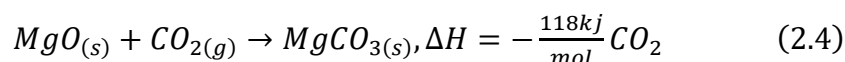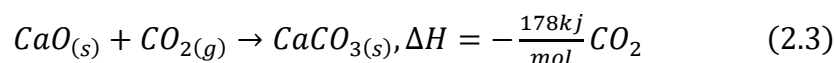
Accelerated carbonation processes have been extensively studied to optimise the storage of CO_2. Researchers have focused on optimizing various operating conditions such as pressure, temperature, liquid-to-solid ratio, humidity of the gas, flow rates of both gas and liquid, particle size, and pre-treatment of the solid material in numerous experimental investigations (Pan, Chang, and Chiang, 2012). Accelerated carbonation can be divided into two main categories which are mineral carbonation and alkaline solid waste carbonation. Mineral carbonation is characterized as a process in which minerals react with CO_2, resulting in the formation of at least one type of carbonate product. On the other hand, utilising alkaline solid waste for the accelerated carbonation reaction can be very effective, especially when these wastes are produced close to the CO_2 emissions source as this approach offers both environmental and economic advantages.

2.7.3 Direct Carbonation

Direct carbonation is a one-step process to convert the CO_2 gas into carbonate. Direct carbonation can be classified into gas-solid carbonation and aqueous carbonation.

2.7.3.1 Gas-Solid Carbonation

The most basic and direct method of carbonation is gas-solid carbonation. In this method, the reaction takes place in a single step, where purified CO_2 gas comes into contact with materials containing calcium and magnesium oxide (Rahmanihanzaki and Hemmati, 2022). This exothermic and slow process results in the formation of carbonates, but the prolonged duration of this reaction is the main obstacle to the practicality of the direct carbonation method. A solid mineral cation source and gaseous carbon dioxide will interact during the dry gas-solid direct carbonation process. This approach has advantages because it has the convenience of utilisation and the ability to reuse

heat produced by the exothermic process. Nevertheless, the reaction kinetics tend to be inadequate for practical industrial applications due to its low efficiency. Since the efficiency of solid-gas single-stage carbonation reaction is unsatisfactory to most researchers, two strategies have been introduced to improve the reaction rate. The first strategy is to conduct the process in the presence of water or water vapour. According to Larachi et al. (2010), an extensive experiment of gas-solid carbonation is conducted involving chrysotile under two different environments which are dry and 10 % H2O atmospheres respectively. These reactions took place between 300 and 1200 °C and under air pressure. The final result is magnesium carbonate hydrate eventually formed in both conditions (Romanov et al., 2015). Notably, the presence of water significantly enhanced the rate of carbonation. The second strategy is to perform the carbonation reaction indirectly into two stages. This is because the gas-solid interactions are shown to be more practical from an energy and financial perspective when carbonating Ca, Mg, or hydroxide. Since Ca- and Mg-silicate minerals do not carbonate directly, this process is known as an indirect carbonation method. Instead, during the first stage of the process, the silicate is converted into an oxide or hydroxide intermediate product. This multi-step process is covered in more detail in the next indirect carbonation section.

2.7.3.2   Aqueous Carbonation

Aqueous carbonation is the carbonic acid route process that involves the reaction of CO_2 at high pressure around 100 to 159 bar in an aqueous suspension with olivine or serpentine (Sanna et al., 2014). The main objective of this aqueous reaction is to create an environment where the appropriate alkali metal oxides, for example, magnesium oxide (MgO) and calcium oxide (CaO) can interact with CO_2 effectively while in the presence of water or water vapour (Rahmanihanzaki and Hemmati, 2022). This is because the reaction kinetics is significantly accelerated with the addition of water. According to Romanov et al. (2015), aqueous mineralisation techniques also take advantage of the enhanced carbonation rates that take place in a mineral slurry submerged in water. A precise method for mineral carbonation has gained significant awareness due to an aqueous carbonation process route

invented by the National Energy Technology Laboratory (NETL). Therefore, it acts as a starting point for research into many aspects of carbonation. When talking about carbonation, the concern is on the reduction of energy consumption and prioritizing affordable techniques that optimise CO_2 use throughout the process. Since aqueous carbonation requires lower temperatures and pressures than solid-gas interactions, this method has repeatedly proven to be a better option. Some specific chemicals can be added to accelerate this reaction. Aqueous carbonation normally is conducted in a single phase or two subsequent processes. The dissolution of CO_2 in the aqueous phase, the precipitation of divalent ions from the mineral matrix, and the eventual deposition of carbonates are the three stages that may be distinguished in the mechanisms of mineral carbonation. The following chemical equations are examples of aqueous carbonation reactions.

$$MO + CO_2 \rightarrow Metal\ Carbonate + Heat \qquad (2.5)$$

$$CO_2(g) + H_2O(l) \rightarrow H_2CO_3(aq) \qquad (2.6)$$

$$H_2CO_3(aq) \rightarrow H + (aq) + HCO_3^-(aq) \qquad (2.7)$$

$$HCO_3^-(aq) \rightarrow H + (aq) + CO_3^{2-}(aq) \qquad (2.8)$$

$$(Ca, Mg)^{2+}(aq) + HCO_3^-(aq) \rightarrow (Ca, Mg)CO_3(s) + H^+(aq) \qquad (2.9)$$

Or

$$(Ca, Mg)^{2+}(aq) + CO_3^{2-}(aq) \rightarrow (Ca, Mg)CO_3(s) \qquad (2.10)$$
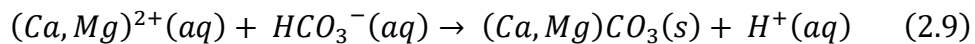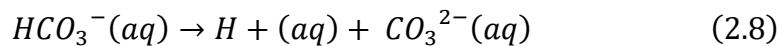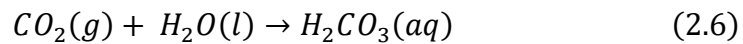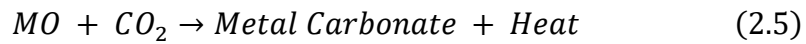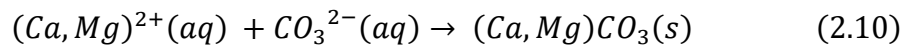
2.7.4 Indirect Carbonation

According to Rahmanihanzaki and Hemmati (2022), the pH range in the direct aqueous carbonation approach is still unsuitable and insufficient for carbonate precipitation as CO_2 normally does not acidify the solution enough to dissolve alkaline particles. Additionally, the process of dissolving minerals needs an acidic environment, which makes CO_2 relatively poorly soluble. A rise in pressure will not greatly speed up the process. The concept of indirect multi-stage carbonation in an aqueous media was consequently introduced. Generally, the carbonation processes that involve more than one stage are

known as indirect mineral carbonation. By utilising acids or other solvents to extract reactive components (Mg^{2+} and Ca^{2+}) from minerals, indirect carbonation typically entails reacting the recovered components with CO_2 in either the gaseous or aqueous phase (Sanna et al., 2014). Pure carbonates can be created indirectly by the removal of contaminants during earlier stages of carbonate precipitation. The extraction of the Ca or Mg reactive components and their interaction with carbon dioxide to generate carbonates are normally the two minimum processes in indirect carbonation. The key to success might be to keep the two reactions distinct as silicate dissolution usually needs a low pH environment while carbonate precipitation needs a higher pH environment. Consequently, indirect carbonation methods like two-stage or pH swing approaches, have been developed (Romanov et al., 2015). The pH swing approach works by adding an acid and a base to the system separately and sequentially, and it can be able to use for further increments of the mineral carbonation rates. The reason behind this is that magnesium and calcium leaching are typically more effective in acidic environments while the required final carbonate synthesis precipitates more readily in basic environments. For instance, Li et al. investigated the carbonization of serpentine using a simulated flue gas before precipitating magnesium carbonate with NaOH. The serpentine that had been heated to 650 °C and then acid-leached produced the best results, with a 98.8 % conversion of the Mg^{2+} in the liquor.

2.7.5 Carbonate Precipitation Using Alkaline Wastes

Conversion of waste minerals into carbonates is one of the alternatives to reduce CO_2 emissions. According to a report from the Intergovernmental Panel on Climate Change (IPCC) in 2005, CO_2 mineralisation by using natural minerals like serpentine and olivine is tough and expensive because the reaction is very slow. This means big reactors or costly methods are required to speed up the process. The preparation stage of these natural minerals by grinding and heating them can also hurt the environment, and at the same time, go against the goal of reducing CO_2 (Pan et al., 2020). Therefore, alkaline waste materials are a better alternative. This is because the waste materials are more reactive instead, and they are also alkaline materials naturally. The alkaline waste materials are often found near factories as they are the majority

of the residue waste of industrial processes. This means that alkaline waste has a ready source. When these materials are used for CO_2 mineralisation, the chemical process becomes more favoured and happens quickly under normal conditions (Pan et al., 2020).

Many different industrial waste sources can be used for mineral carbonation, with a variety of properties and amounts available. In this part of the discussion, two types of alkaline waste will be discussed which are steel slag and cement wastes.

2.7.5.1 Steel Slag

Steel slags are a type of waste material produced during steel manufacturing processes. They are widely available and hold the potential to be used in mineral carbonation. The use of steel slag in carbonation can bring several advantages, including reducing the basicity (pH level), stabilizing swelling, and decreasing the leaching of heavy metals (Bodor et al., 2013). Various methods of making steel led to various kinds of steel slag, such as those resulting from the blast furnace, basic oxygen furnace, electric arc furnace, and ladle furnace processes.

According to Rahmanihanzaki and Hemmati (2022), the iron and steel industry is known for its environmental impact, contributing significantly to global energy consumption which is about 22 % of total industrial energy consumption and with CO_2 emissions of approximately 6 -7 % of total global CO_2 emissions. This industry plays a significant role in directly reducing CO_2 through mineralisation using alkaline waste, with iron and steel alone contributing to 43.5 % of this reduction. Iron and steel slag also contribute notably to indirect carbon reduction, making it a crucial element in the effort to mitigate carbon emissions (Pan et al., 2020).

Steel slag represents an alternative to natural minerals due to its high alkaline potential. This waste material holds several advantages over other alkaline waste materials. For example, the fine particle size of steel slag eliminates the need for grinding and milling, easy accessibility of steel slag and proximity to CO_2 emission sources, low transportation costs, and strong reactivity due to its chemical instability. Moreover, the porous structure of

steel slag enhances the reactivity of alkaline materials when compared to natural alkaline substances (Rahmanihanzaki and Hemmati, 2022).

As mentioned before, the utilisation of steel slag for carbonate mineralisation offers various benefits. It reduces waste production and the costs associated with waste disposal. Instead of being a burden, the waste is transformed into a valuable resource. Additionally, this process contributes to a reduction in CO_2 emissions and helps to combat climate change. In summary, steel slag shows substantial promise in terms of its practical advantages and environmental benefits when used in carbonate mineralisation processes.

2.7.5.2 Cement Waste

Cement stands out as another type of industrial waste that represents an effective alternative alkaline material to replace natural minerals in the carbonation process. Two major sources of CO_2 emissions in industrial sectors are the steelmaking and cement industries. These industries release huge amounts of alkaline solid waste due to their energy-intensive and resource-intensive processes. Remarkably, a substantial amount of CO_2 is emitted during cement production, accounting for approximately 90 % of total emissions from global industries and 5% of total emissions resulting from industrial activities and fossil fuel incineration worldwide (Rahmanihanzaki and Hemmati, 2022). Information from the International Energy Agency (IEA) suggests that producing 1 kg of cement results in the production of 0.81 kg of carbon dioxide.

Cement waste has a significant role in directly reducing CO_2 emissions through mineralisation using alkaline waste as well. Specifically, cement waste contributes to 16.3 % of this reduction. Additionally, it also contributes notably to indirect carbon reduction. For instance, it's estimated that around 3.7 gigatons of CO_2 emissions could be indirectly prevented by reusing carbonated products as construction materials. Among various waste materials, carbonated cement or concrete waste contributes the most to indirect CO_2 reduction, followed by carbonated coal combustion products, iron and steel slags, and mining wastes (Pan et al., 2020).

Cement waste that is suitable for carbonation includes materials like cement mortar, cement kiln dust, and construction cement scraps. One interesting characteristic of cement is its high alkaline potential. Typically, CO_2 reacts naturally with cement in building materials or structures containing concrete when exposed to the atmosphere. Although this process is slow and can lead to damage, it demonstrates the potential of cement for carbonation (Rahmanihanzaki and Hemmati, 2022).

According to Rahmanihanzaki and Hemmati (2022), the process of carbonation with cement waste consists of several steps. First, waste cement powder dissolves in water. Then, CO_2 interacts with the solution, and this is the step that takes the most time. Following that, chemical reactions between CO_2 and calcium ions lead to the precipitation of CaCO3 (calcium carbonate). The carbonation reaction can be divided into three stages:

(i)   dissolution of cement waste.

(ii)   adsorption of CO_2 and formation of carbonate ions.

(iii)   chemical reaction and formation of the precipitate.

Similar to steel slag, utilising cement waste offers advantages such as reducing waste production and disposal costs, turning waste into valuable products, and decreasing CO_2 emissions. Cement waste serves as a feasible alternative for alkaline materials in the carbonation process, contributing to both direct and indirect carbon reduction efforts.

2.8   Type of Analysis Method

The purpose of carrying out analysis methods in the experiment is to obtain relevant data and information about the sample. The crucial information such as chemical composition, chemical properties, and physical properties can be obtained by conducting the experiments. Therefore, different analysis methods should be used to get all the required information due to the different analysis methods may have their functions to obtain specific information only. Besides, comparison can be done through the results obtained from different analysis methods as well. This ensures the accuracy of the information obtained. The examples of analysis methods used are XFD, TGA, SEM, and EDS.

2.8.1 X-ray Diffraction (XRD)

X-ray diffraction (XRD) is a powerful non-destructive technique used to examine crystalline materials. XRD can provide insightful information about the materials' structures, phases, preferred crystal orientations (texture), and various structural parameters like average grain size, crystallinity, strain, and crystal defects (Bunaciu, Udriştioiu and Aboul-Enein, 2015). Due to the fact the wavelengths of X-rays that are similar to atomic dimensions, they can be used to retrieve information about atomic structures. For instance, X-ray diffraction (XRD) enables the analysis and characterization of atomic positions, their configurations inside each of the cells, and the distance between atomic planes (Ali, Chiang, and Santos, 2022).

Minerals, polymers, plastics, metals, semiconductors, ceramics, and even solar cells can all be studied with this non-invasive technology. The application of XRD is widely used in a variety of sectors, including microelectronics, aircraft, and power generation. When a monochromatic X-ray beam scatters from the sample's lattice planes at particular angles, creating constructive interference and peak emergence, hence produces the X-ray diffraction patterns. The X-ray diffraction pattern serves as a distinctive identity for the atomic arrangements in a given material since the intensity of these peaks varies based on the distribution of atoms inside the lattice (Bunaciu, Udriştioiu, and Aboul-Enein, 2015).

The limitation of XRD is some complex crystal formations and related diffraction patterns are still unfathomable despite its numerous applications, which poses challenges for both Laue's and Bragg's theories. Although the majority of the features in a diffraction pattern can be explained by conventional kinematical and dynamical theories, they come with several limitations too. When deviating from the Bragg condition, dynamical theory encounters difficulties, while kinematical theory poses issues with statistics, particularly in powder diffraction where the quantity and consistency of observed peaks are relevant (Fewster, 2023). Kinematical theory, rather than dynamical theory, which is crucial at the Bragg condition, is primarily followed in single crystal research. Moreover, XRD has another limitation which is the requirement of sample powdering for optimal results. This requires labour-intensive, time-consuming, and costly procedures such as

careful sample splitting, milling, and particle-size fractionation (Ali, Chiang, and Santos, 2022). XRD analysis becomes more difficult due to the lack of peak contrast in diffraction patterns and the occurrence of overlapping interference patterns. The efficiency of the XRD method might also be affected by complex procedures including sample preparation, K-value calculation, and calibration curve development (Ali, Chiang, and Santos, 2022). Therefore, additional study is essential to improve the overall XRD testing and analysis methods, especially for complex mineralogical structures.

2.8.2   Thermogravimetric Analysis (TGA)

Thermogravimetric Analysis (TGA) is a widely used method for precise monitoring of the weight loss in a small sample subjected to controlled temperature changes and heating rates (Felix et al., 2022). The sample mass for isothermal testing or the temperature for non-isothermal tests are commonly represented graphically using thermograms. These thermograms can be quickly processed to provide first-differential thermogravimetric (DTG) weight-loss profiles that help in identifying the distinct stages of decomposition and the temperatures associated with each one (Felix et al., 2022). TGA is commonly used as the first step when there is a need to find out the mass balance between cellulose, hemicellulose, and lignin in lignocellulosic biomass, proximate analysis, or to analyse the thermal breakdown of a given sample. Additionally, Felix et al. (2022) stated that TGA provides essential data for reaction kinetics modelling since it permits neglecting internal mass transfers and temperature gradients within the sample. This is especially beneficial for optimizing reactor designs with computational fluid dynamics (CFD).

TGA studies are conducted in a thermogravimetric analyser, where the sample is set up and placed on a precision balance within a furnace. The experiment can be run in either isothermal or non-isothermal circumstances, with the furnace helping to control the temperature (Escalante et al., 2022). To regulate the environment, a purge gas which may be inert or reactive is passed through the sample. Inert gases are frequently utilised in conventional TGA investigations due to the lack of oxygen during pyrolysis. Although argon and helium are also commonly utilised inert gases, nitrogen is the preferred option.

The analyser is typically connected to a computer so that data can be recorded while the experiment is being conducted to observe the change in sample mass with temperature. According to Escalante et al. (2022), the data are often given as TG curves, which display the sample's percentage weight loss (wt.%) as a function of rising temperature (T), and the weight drops as the temperature rises because of mass loss brought on by the sample's thermal deterioration. As seen, colder temperatures are the conditions where most of the decomposition takes place. By tracking the changes in sample mass, TGA is useful for characterising material changes that occur with temperature, both physically and chemically (Escalante et al., 2022). Although the TGA's fundamental idea is relatively simple, it has a wide range of applications and is used as the first stage in the investigation of several reactions, processes, and phenomena, including heat and mass transfer (Saadatkhah et al., 2019). However, conventional TGAs have limitations in the field of sample size and the rates of heat and mass transfer. For instance, Saadatkhah et al. (2019) mention that heating rates within the sample may not be fast enough to ensure isothermal conditions, leading to poor mass transfer and the creation of concentration gradients in both radial and axial directions for larger samples that are larger than 50 mg. These limitations increase uncertainties when deriving kinetic parameters from conventional TGA analyses. Additionally, the majority of TG analysers are only able to operate at temperatures up to 900 ℃. Some materials may be subjected to procedures or uses that call for exposure to temperatures as high as 1600 ℃, such as the sintering of metal powders or the burning of industrial waste. Therefore, new micro-TGA reactors, like the FB-TGA, IHFB-TGA, and MW-TGA, have been developed to overcome these limitations. These reactors are designed with the purpose of more closely resembling industrial processes and removing restrictions on heat and mass transmission as well as operating temperature and pressure (Saadatkhah et al., 2019).

2.8.3   Scanning Electron Microscopy (SEM)

Generally, there are two available microscopy techniques which are optical microscopy and scanning electron microscopy (SEM). The former technique, optical microscopy is an older technique that has been applied for the past two centuries in a relatively simple form with limited capabilities (Mohammed and Avin Abdullah, 2019). On the other hand, scanning electron microscopy (SEM), also known as SEM analysis or SEM technique, has gained widespread adoption across various fields.

SEM is applied widely due to its ability to produce highly magnified images that reveal detailed information such as size, shape, composition, crystallography, and various physical and chemical properties of a specimen (Ural, 2021). SEM is one of the effective methods for analysing both organic and inorganic materials on a wide scale which has a range from nanometres to micrometres. SEM also can achieve higher levels of magnification, reaching up to 300 000 × and even up to 1 000 000 × in some modern models. This enables precise imaging of a wide range of materials. In conjunction with SEM, energy-dispersive X-ray spectroscopy (EDS) is often employed to provide qualitative and semi-quantitative results. The combination of these two techniques helps provide essential insights into the composition of scanned specimens, information that cannot be readily obtained through conventional laboratory tests (Mohammed and Avin Abdullah, 2019).

The theory behind SEM is directing the high-energy electrons at a sample and the resulting emissions of electrons (secondary electron and backscattered electron) and X-rays from the sample are then analysed. Secondary electron refers to the electron from the inelastic collision between electron and sample while backscattered electron is the redirected electron results from elastic collision between emitted electron and sample. According to Akhtar et al. (2018), these emissions provide valuable information about various aspects of the material being examined, including its topography (surface features and texture), morphology (shape and size of objects), composition (elements and compounds present in the material), and crystallography (the arrangement of atoms within the material). By using high-energy electrons and analysing the emitted signals, SEM allows for a detailed

characterization of a material's physical and chemical properties. SEM machine consists of several main components which are:

(i) Electron gun (a source to generate electrons).

(ii) Electromagnetic lenses.

(iii) Deflection system (scan coils).

(iv) Electron detector (to detect secondary electrons and backscattered electrons).

(v) Chamber (to place the sample).

(vi) Computer system (to view images and control the electron beam).

2.8.4 Energy Dispersive X-ray Spectroscopy (EDS)

For more than 50 years, electron probe microanalysis (EPMA) has been a popular analytical technique, particularly for determining the elemental composition of solid-state materials at the micrometre scale (Hodoroaba, 2020). By using an electron beam to excite the sample, this technique examines the X-rays that were released, which have specific energies for each element. Energy-dispersive X-ray spectroscopy (EDS/ EDX) is used in EPMA as a precise quantitative technique for homogeneous samples with flat, smooth surfaces. Additionally, it is a quick and nearly non-destructive method for qualitative chemical analysis such as comparing the relative concentration of elements or determining the similarity of related samples (Hodoroaba, 2020). EDS can detect almost all elements in the periodic table with only hydrogen and helium being the sole exceptions as they fail to emit the X-ray.

Energy Dispersive X-ray (EDS/ EDX) microanalysis is known as an elemental analysis technique that is linked to electron microscopy, by relying on generating characteristic X-rays through the interaction of incident electron beam electrons with the sample's atoms (Scimeca et al., 2018). Two types of electron interactions occur during the analysis: elastic scattering and inelastic scattering. Elastic scattering involves a change in the electron's direction without a significant energy loss due to interactions with the nucleus of the material, while inelastic scattering results in energy loss without a noticeable change in direction (Scimeca et al., 2018). This is usually caused by interactions with both the bound electrons and the nucleus in the atoms. Elastic

scattering events primarily determine the shape of the interaction volume, while inelastic scattering events mainly influence its size. However, ionised atoms release distinctive X-rays when they revert to their ground state. These X-ray photons possess the energy that is specific to the element and are determined by the energy difference between the two orbitals that are involved in the transition. A photon-energy sensitive detector can monitor different wavelengths of X-ray emissions, and these X-rays reveal information about the components present in the material.

The limitation of EDS is that EPMA uses X-ray spectrometry to detect elements, but it is not able to distinguish between ionic and non-ionic species. Besides, due to the significant X-ray and electron absorption by air molecules, all materials must be examined in a relatively vacuumed atmosphere (Scimeca et al., 2018). Although inter-element interference, also known as peak overlap, can hinder X-ray detection, it usually has minor impact on it and can make elemental analysis more difficult.

CHAPTER 3

METHODOLOGY AND WORK PLAN

3.1   Introduction

The methodology used in this report refers to a systematic method to collect and analyse data, conduct experiments, and perform other necessary procedures to achieve the aim and objective of this study. In this chapter, a flowchart that shows the overall methodology, and the materials and equipment used are included.

3.2   Flowchart

In this section, the methodology of this study is summarized in a flowchart as shown in Figure 3.1 below. Firstly, the methodology starts with the sample collection and preparation. The sample is the EAF slag from Penang. Next, the sample is characterised to identify and determine its chemical composition, crystalline structure, and other properties. After this, the concrete casting starts and continues with laboratory testing such as compressive tests once the concrete is cured. Essential experimental data are collected. Then, the data collected during the experiments undergoes analysis by using XRD, SEM, EDS, and compression tests to be used in the discussion and conclusion. Lastly, a conclusion for the carbon capture capacity of EAF slag is drawn by summarising the results and findings.
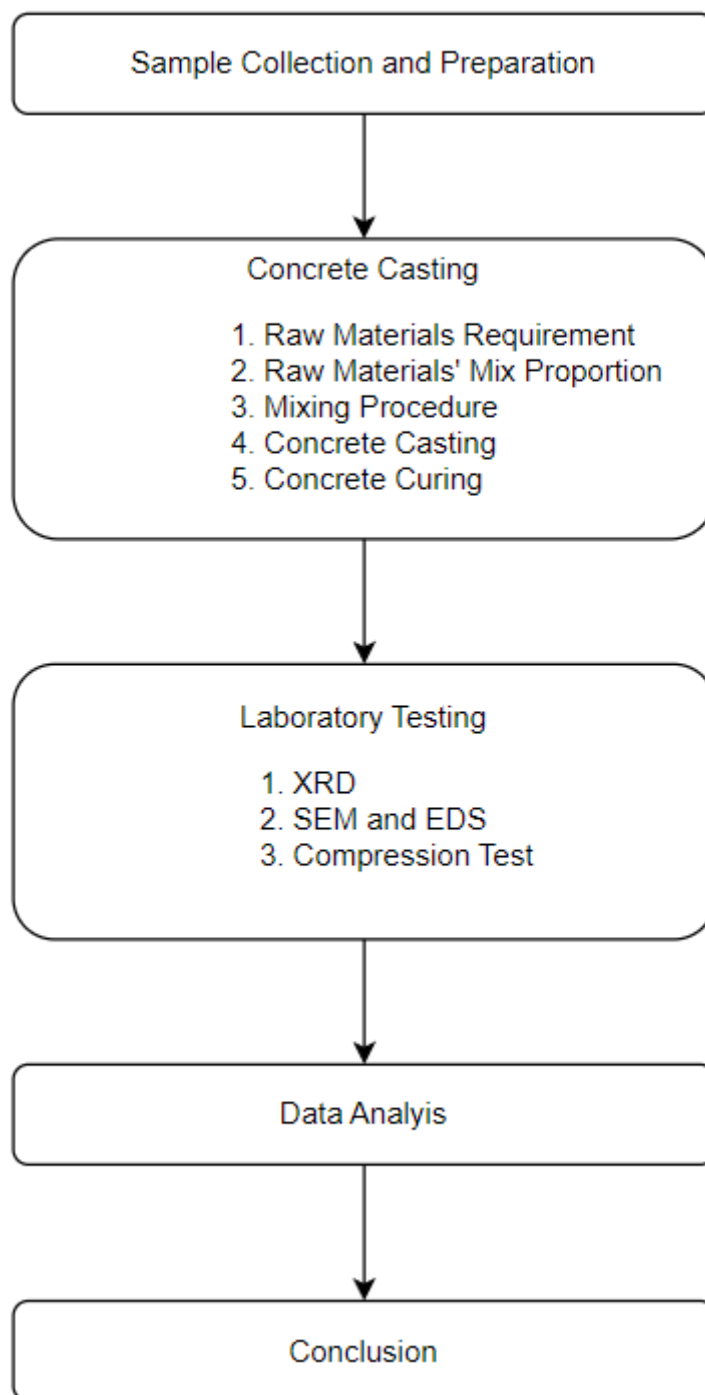
Figure 3.1: Flowchart of Methodology.

3.2.1 Sample Collection and Preparation

The study utilised EAF slag as the sample to evaluate the potential of carbon capture of local waste streams. The final sample selected is from Penang states. After sample selection, the samples underwent a rigorous step of preparation. This required crucial processes including oven drying and sieving to classify the raw EAF slag into the appropriate particle size range and get rid of undesirable pollutants. The initial step in sample preparation is oven drying, which eliminates the moisture inside the raw EAF samples. The slags are placed into the oven for one day before conducting the sieving process. The sieving machine conducts the sieving process. The sieving machine will shake continuously for about 15 min and the sand will pass through several sizes of sieve such as 6.3 mm, 5.0 mm, 4.75 mm, 3.35 mm, 2.36 mm, 1.18 mm, and pan. The slags collected in each sieve and the final pan are placed into different containers according to the particle size range. Figure 3.2 shows the setup of a sieve and pan, and Figure 3.3 shows the setup of a sieving machine.

Figure 3.2: Setup of Sieves and Pan.

Figure 3.3: Setup of Sieving Machine.

After sample preparation, each sample was properly labelled with the necessary details to prevent any confusion or mistakes. This comprehensive labelling process is an essential safety safeguard to guarantee that the right sample is used throughout the experiments.

3.2.2   Concrete Casting

After sample collection, preparation, and characterization, the sample is used as a partial replacement of fine aggregate in concrete casting. The final products of this step are ten sets of concrete cubes, with each set of three. Besides, one of the concrete cubes sets without adding the steel slag is acting as the control set. The remaining nine sets of concretes can be classified by their particle size and the percentage of steel slag replacement as shown in Table 3.1 below.

Table 3.1:   Concrete Categories.

Particle size (mm)	Percentage of steel slag replacement (%)		
	15	30	45
7- 4.75	3	3	3
4.75 – 2.36	3	3	3
2.36 – 0.8	3	3	3

3.2.2.1 Raw Materials Requirement

The raw materials used in this experiment to produce the concrete are Ordinary Portland Cement (OPC), fine aggregates (sand), water, and EAF slag. Figure 3.4 shows the raw materials used in this experiment.

(a)

(b)

(c)

(d)

Figure 3.4: (a) Cement (b) Water (c) Sand and (d) EAF Slag.

The OPC cement used in the concrete casting is Castle Simen Portland Komposit from YTL Cement, with each bag weighing 25kg. The slag used is sourced from EAF in Penang and has undergone a screening process to achieve the desired particle size range. Sand is used as a fine aggregate in concrete casting and has also undergone oven drying and screening to remove contaminants. Water plays a crucial role as a mixing agent in the concrete casting process. The water used must be free of contaminants and meet drinking water standards; therefore, this study uses water from municipal water systems to meet these requirements.

3.2.2.2 Raw Materials' Mix Proportion

It is critical to determine the exact weight of each raw material for the reason to get the desired workability in the concrete mix. In this project, a water-cement ratio of 0.55 is used, and cement and sand are used in equal amounts. The quantity of raw materials is increased by 30 % to allow for mixing-stage waste. The absolute volume method is used to calculate the percentage of each material. The single concrete's weight and proportion of different raw materials of control set and concrete with 15 % EAF slag replacement and 7-4.75 mm particle size are shown in Tables 3.2 and 3.3.

Table 3.2: Weight of Raw Materials (control set).

Type of Raw Materials	Proportion	Weight (kg)
OPC	1	3.97
Sand	1	3.97
Water	0.55	2.18
Total	2.55	≈ 10.125

Table 3.3: Weight of Raw Materials (with 15 % EAF slag and 2.36 – 0.8 mm).

Type of Raw Materials	Proportion	Weight (kg)
OPC	1	3.878
Sand	0.850	3.297
Water	0.550	2.133
Steel Slag	0.249	0.817
Total	2.649	≈ 10.125

3.2.2.3 Mixing Procedure

The mix proportion for each material must be determined before commencing the concrete mixing process. In a cement mixing container, the raw materials like cement, sand, and steel slag are blended. The dry mixture is then gently hydrated with water until it reaches an even consistency. The processes involved in mixing concrete are shown in Figure 3.5. By carrying out the fresh density test, the density of concrete is ensured to achieve the target.

Figure 3.5: Concrete Mixing Process.

3.2.2.4 Concrete Casting

Once the concrete mix achieves the desired density, the concrete mix is then poured into cube moulds with dimensions of 150 mm × 150 mm × 150 mm for casting purposes. The cube moulds are coated with a thin layer of oil before the concrete mix is poured to ease the demoulding step the next day. A piece of paper is also placed on the bottom opening of the mould as an identity to differentiate it from other concrete cubes which all gather in a water tank for curing later. The pouring of fresh concrete mix is separated into three layers and each layer was evenly tamped with a tamping rod to ensure the release of any trapped air bubbles. Figure 3.6 shows the preparation process of concrete moulds and Figure 3.7 shows the concrete casting process. After that, the concrete mixture was allowed to dry and set for a full 24 hr.

Figure 3.6: Preparation of Moulds.

Figure 3.7: Concrete Casting.

3.2.2.5 Concrete Curing

After 24 hr had passed, the demoulding procedure was started. The concrete cubes were put in a water tank for water curing to encourage a good cure. The specimens were completely submerged in water throughout the whole curing process, which took place in a tank that was kept at a constant temperature of 16 to 27 ℃. The concrete cubes were taken out of the water tank after 28 days of water curing to perform further analysis. Figure 3.8 below shows the concrete curing process.

Figure 3.8: Concrete Curing.

3.2.3 Laboratory Testing

Laboratory testing such as compression test, XRD, SEM, and EDS is conducted in this step to collect necessary data such as chemical properties, physical properties, and mineral composition of the sample. For example, XRD analyse the sample by analysing the X-ray diffraction patterns which is a distinctive identity for the atomic arrangements in a given material results from the monochromatic X-ray beam scatters from the sample's lattice planes

at particular angles (Bunaciu, Udriştioiu and Aboul-Enein, 2015). Besides, SEM is used to produce a highly magnified image of the sample. Useful information such as the size, shape, composition, crystallography, physical properties, and chemical properties of the sample can be obtained through the image (Ural, 2021). EDS is usually coupled with SEM to result in a better analysis, and it is useful in comparing the relative concentration of elements or determining the similarity of related samples (Hodoroaba, 2020). Compression test is conducted to evaluate the compressive strength of the EAF concrete.

3.2.3.1 XRD

XRD is used to examine crystalline materials and helps in revealing the atomic structure, analysis and characterization of atomic positions, their configurations inside each of the cells, and the distance between atomic planes (Ali, Chiang, and Santos, 2022). The first step to conduct XRD is to ground the concrete sample into powder form as shown in Figure 3.9.

Figure 3.9: Grinding Sample into Powder Form.

The resulting powdered sample is placed on a sample holder once the steel slag or concrete cubes have been completely ground. A glass slide is then used to ensure the sample is flat and to prevent spillage when the sample holder is tilted during analysis. Once the sample is firmly secured, the sample holder is handed to a laboratory technician who inserts it into the XRD

instrument. The instrument is then set to scan the sample holder over a continuous scan mode, a scan speed of 2.000 (°/min), and a scan range of 5° to 85°, to facilitate comprehensive data acquisition. The XRD analysis begins with the instrument scanning the sample holder from the initial angle to the final angle. X-ray diffraction patterns, which provide insight into the crystal structure and composition of the sample, are recorded at various angular intervals.

3.2.3.2 SEM and EDS

In this study, the SEM and EDS are conducted both for the concrete sample and the EAF slag sample. The EAF slag sample undergoes SEM and EDS analyses before concrete casting. This test is to examine the composition of raw EAF slag samples. Figure 3.10 shows the sieved EAF slag samples that were packed inside the plastic bags according to different particle size ranges to undergo the first test before concrete casting.

Figure 3.10:   EAF Slag Samples for First Test after Carbonation.

For the concrete sample, all the concrete cubes are crushed into small pieces as shown in Figure 3.11 below before carrying out the SEM and EDS tests.
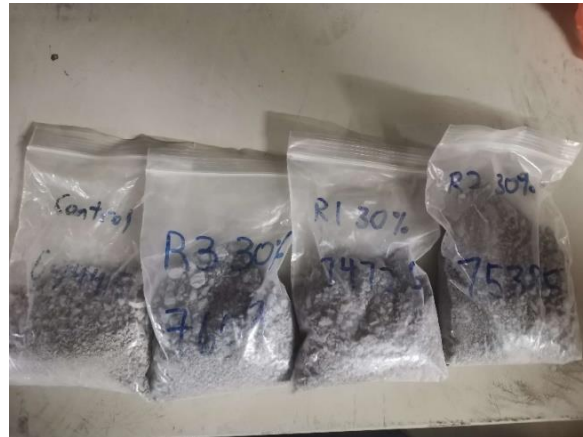
Figure 3.11:   Small Concrete Particle Samples for SEM and EDS Tests.

Although the SEM and EDS do not require the sample to be grounded into powder form, there is a size limitation for the sample as the samples are taped on a small platform with numbers on it for better identification of the sample as shown in Figure 3.12. The oversize particle will affect the accuracy of the test and get undesired results.

Figure 3.12:   Sample Platform and Holder for SEM and EDS test.

This platform is then placed in the SEM. The SEM machine scans the surface of the sample with a focused electron beam, producing detailed images of how it looks. Meanwhile, the EDS machine captures special X-radiation emitted by the sample when it's hit by the electron beam. These X-rays are an indication of what elements are in the sample and how much of each there is. The EDS machine examines all the X-ray information to figure out which elements are present and how much of each. The operators doing the testing can pick out areas they're interested in on the SEM images and check for specific elements or use a special tool that shows where different elements are in the sample.

Finally, the SEM images and EDS information are viewed and studied to understand the sample's topography, morphology, composition, crystallography, and other characterizations.

3.2.3.3   Compression Test

Besides, the hardened concrete properties test conducted in this experiment is called the compression test. The test is carried out over 28 days for all the concrete cubes. The objective of compression tests is to assess how a material responds when subjected to crushing loads. These tests include using platens or specialized fixtures on a universal testing machine to apply compressive pressure to a test specimen, which is often shaped like a cuboid or a cylindrical object. In this experiment, this test is being done to determine the maximum load that the specimens can withstand before failing. Before the start of testing, a few configurations must be made on the display panel before operating the machine. Next, the surface of the compression machine is cleaned to avoid dust and disturbance which may affect the accuracy of results. Then, the specimen needs to be placed in the middle of the testing apparatus to guarantee accurate findings during the compression test. A constant axial load will be applied by the compression machine until the specimen inevitably cracks as shown in Figure 3.13 and the maximum load is recorded.

Figure 3.13:   Cracking during Compression Test.

3.2.4   Data Analysis

Data results from previous tests such as XRD, SEM, EDS, and compression test is collected. The results are then used for further analysis and interpretation of the carbon capture capacity of EAF slag and the compressive strength of concretes. Tables and graphs are plotted in this step to aid in visualisation and to enhance the understanding of readers.

3.2.5   Conclusion

The final step in the methodology of this study is to conclude. All the discussions that are based on the experiment results are taken into consideration. A precise statement for the study is given to cover all the key points and highlights in the discussion. The carbon capture capacity of the EAF slag is also proposed in this section.

3.3   Equipment Used

3.3.1   X-ray Diffractometer (XRD)

X-ray diffraction (XRD) is a powerful non-destructive technique used to examine crystalline materials. As mentioned before, XRD is useful for analysing the material's properties such as revealing the structures, mineralogical phases, crystal orientation, and other structural parameters of the samples (Bunaciu, Udriştioiu, and Aboul-Enein, 2015). This eventually helps to find out the formation of carbonate minerals and aids in evaluating their stability and efficiency. XRD can analyse various types of materials including minerals, polymers, plastics, metals, semiconductors, ceramics, and even solar cells. XRD requires a sample in fine powder form, so grinding the sample into the required particle size is necessary. Therefore, XRD is suitable to use in the analysis of GGBS in this study. The XRD machine used is known as an X-ray diffractometer, specifically the Shidmazu brand with the model's name XRD-6000. This X-ray diffractometer consists of five components, including an X-ray tube, an X-ray generator, a goniometer, a detector, and a casing. Figure 3.14 shows the X-ray diffractometer used at Universiti Tunku Abdul Rahman.

Figure 3.14:   X-ray Diffractometer (Universiti Tunku Abdul Rahman, 2018).

3.3.2   Compression Machine

In the field of concrete construction, compression machines are one of the essential tools used for testing concrete compressive strength. The compression machine is used in the construction industry to assess the quality of concrete. It determines the compressive strength of concrete by applying controlled compressive forces to specimens until the specimen cracks under maximum load. It can also assess the compressive strength of various materials including bricks, stone, and metals. Compression machines are available in a range of sizes, capacities, and types. The two main types are manual and digital. Manual compression machines require skilled operators to manage load applications, whereas digital counterparts operate automatically and require minimal training to use. Compression testing machines provide vital information about the durability and suitability of the material for various construction applications by measuring the resistance of the concrete to these forces. Figure 3.15 shows the compression machine used in Universiti Tunku Abdul Rahman.

Figure 3.15:   Compression Machine.

3.3.3 Scanning Electron Microscope (SEM)

SEM is a useful technique to visualize the topography, morphology, composition, and crystallography of a material (Akhtar et al., 2018). This detailed information can be revealed through the high-magnified image produced by SEM. SEM works by directing the electron beam to the sample surface and then analysing the resulting emissions of secondary electrons, backscattered electrons, and X-rays from the sample surface. EDS is always coupled with SEM to produce qualitative and semi-quantitative results. The reason behind this is EDS works in similar ways to SEM in which EDS is linked to electron microscopy, by relying on generating characteristic X-rays through the interaction of incident electron beam electrons with the sample's atoms (Scimeca et al., 2018). The machine used to conduct the SEM is known as the scanning electron microscope, specifically the Hitachi brand with the model's name S-3400N. A scanning electron microscope consists of several components, including an electro gun, electromagnetic lenses, a deflection system, an electron detector, a chamber, and a computer system. Figure 3.16 shows an example of the scanning electron microscope used at Universiti Tunku Abdul Rahman.

Figure 3.16:   Scanning Electron Microscope.

3.4   Main Material

The main material used in this study is the electric arc furnace (EAF) slag. EAF slag is selected as the sample in this study to evaluate the carbon capture potential of the local waste stream. There are ready sources for EAF slag since it is a by-product produced during the steelmaking process. These steel slags are waste, but they can be used in carbonation to capture the carbon dioxide gaseous and can bring several advantages, including reducing the basicity (pH level), stabilizing swelling, and decreasing the leaching of heavy metals (Bodor et al., 2013). Since the utilisation of EAF slag for carbon capture offers various benefits, it is selected as the main material in this study.

3.5   Summary

In summary, the methodology in this study comprises four major steps which are sample collection, preparation, and characterization, mineralisation experiment, data analysis, and conclusion. To improve the workflow, some minor steps are introduced into the major step. The sample material used in this study is EAF slag, originating from the local factory found in Penang. The equipment used in this study includes an X-ray diffractometer, compression machine, and scanning electron microscope. Since all the equipment is available in Universiti Tunku Abdul Rahman, this eventually helps to save the cost and time compared to analysing other laboratories.

CHAPTER 4

RESULTS AND DISCUSSION

4.1   Introduction

In this chapter, the data collected from the experiments conducted in the laboratory are summarized in tables and graphs to facilitate an easier understanding of the results. This chapter is concerned with presenting the results and explanation of the experiments conducted, for example, the EDS test, SEM test, XRD test, and compression test to evaluate the carbon capture potential, the optimum particle size range, and compressive strength of the EAF slag concrete samples. These tests help in providing necessary information on the EAF slag to determine its potential in achieving the aim and objectives of this study.

SEM tests produce highly magnified images that can reach up to 300 000 x and even up to 1 000 000 × to provide the sample's detailed information such as size, shape, composition, and crystallography. The image produced helps the researchers to have a clearer picture of the internal structure of the samples. EDS test is always used along with the SEM test for determining the elemental composition of solid-state materials at the micrometre scale (Hodoroaba, 2020).

XRD analyses the crystal structure of materials. By shining X-rays through a sample, XRD measures the angles and intensities of the X-rays scattered by the sample's atomic structure. This information can reveal details about how atoms or molecules are arranged within materials, help identify which type of crystal structure is present, determine which crystal phase of material is present, and study defects or imperfections in crystal.

Compressive strength is one of the important parameters of mechanical properties of concrete other than tensile, flexural strength, shear strength, and modulus of elasticity. The compressive strength of concrete is the only mechanical properties that are conducted due to the limitation and scope of this study.

4.2   Compression Test

4.2.1   EAF Slag

As one of the objectives of this report, the compression test was carried out on both normal concrete and EAF slag concrete to evaluate and compare their compressive strength. The results of the compression test are discussed in this section. The discussion in this section focuses on comparing the compressive strength of the two types of concrete, analysing the effect of the EAF slag particle size on the compressive strength, and assessing the effect of varying the percentage of EAF slag used as a replacement for fine aggregate. Besides, the comparison of BOF slag concrete and EAF concrete compressive strength will also be discussed in this section to study about the properties and understand their differences.

The average compressive strength of the concrete under different particle sizes and the percentage of replacement are summarised in Table 4.1 to facilitate the interpretation of the data. Each category consists of three concrete cubes; the results recorded represent the average compressive strength of these cubes. Nine sets of categories for EAF slag concrete result in a matrix of three by three, formed by the particle size and percentage replacement parameters. Of these categories, the R3 group (7.62-4.75 mm) with 45 % replacement has the highest compressive strength. This indicates that larger particle sizes and higher percentages of replacement improve the mechanical properties of concrete in terms of compressive strength. In addition, a bar chart illustrating the range of particle sizes and the compressive strength of the concrete at different percentages of replacement has been plotted (see Figure 4.1) and shows a trend of increasing strength with higher percentages of replacement within the same group of particle size ranges. This suggests that EAF slag is effective in improving the strength of concrete, with higher replacement percentages resulting in greater strength gains. This is because the presence of EAFS in concrete offers better behaviour in its physical and mechanical properties due to the angularity and the rougher texture of the artificial aggregate, which gives a stronger adhesion to the cement matrix and improves its ITZ (Rojas et al., 2023). Furthermore, the particle size of the EAF slag also influences the compressive strength of the concrete, as shown in Figure 4.1. For instance, R1 (2.36 mm- 0.08 mm)

concrete has a compressive strength of 684.50 MPa, much lower than the compressive strength of R3 concrete, which is 879.90 MPa even at the same replacement rate of 45 %. The results in Table 4.2 show that the average compressive strength of R1, R2 and R3 concrete is higher compared to the control set further supporting the effect of particle size on the compressive strength of concrete. Referring to Table 4.1, it can be seen that most of the EAF slag concretes typically exhibit superior compressive strength compared to the base concrete, with an increase in strength ranging from 1.60 % to as much as 45.9 %, with an exception which is R1 15 concrete that does not follow this trend. The results are in line with previous research done by Abu-Eishah, El-Dieb and Bedir (2012) which has indicated that EAF steel slag has favourable properties for use as an aggregate in construction, resulting in the production of high-strength concrete compared to conventional mixes. His research showed that the 28-day compressive strength achieved exceeded the specified strength requirements, reaching 60 MPa, 80 MPa and 100 MPa for concrete mixes designed for strengths of 30 MPa, 50 MPa and 70 MPa respectively. The observed increase in strength ranged from 42 % to 100 %. In addition, for mixes containing supplementary cementitious materials (SCM), the strength increases in a range from 70 % to 80 %. This increment, facilitated by the rough and porous surface texture of the EAF steel slag particles, is attributed to the strong bond between the cement/mortar matrix and the EAF steel slag aggregate particles (Abu-Eishah, El-Dieb and Bedir, 2012).

Table 4.1: Average Compressive Strength of EAF Slag Concrete under Different Particle Size and Percentage of Replacement.

| Particle size Range | Average Compressive Strength (MPa) | | | |
| | Percentage of steel slag replacement (%) | | | |
	0	15	30	45
R1	-	445.80	569.87	684.50
R2	-	664.63	778.67	842.93
R3	-	734.40	827.73	879.90

Control	557.80	-	-	-
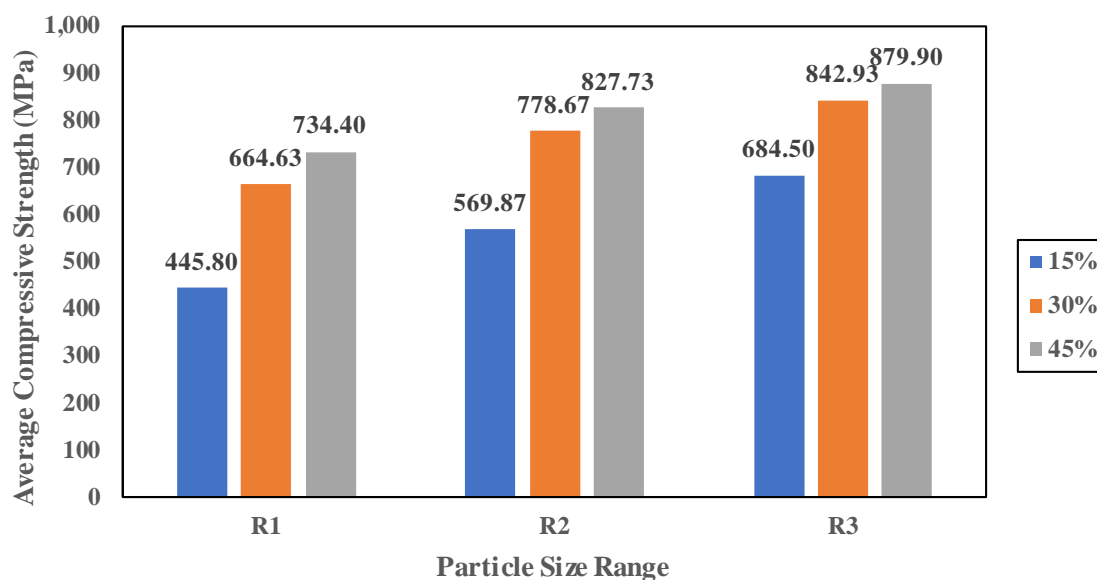
Figure 4.1: Average Compressive Strength of EAF Slag Concrete under
Different Particle Size Range and Percentage of Replacement.

Besides, an analysis of the effect of the particle size and the percentage of replacement of EAF slag on the compressive strength of the concrete is shown in another graph (Figure 4.2), which highlights the percentage of replacement as the most influential factor on the compressive strength. In Table 4.2, concrete with a 45 % replacement of EAF slag achieves the highest compressive strength (814.01 MPa) followed by the concrete with R3 particle size range EAF slag has the second highest compressive strength of 802.44 MPa. This is in line with previous studies, which found that replacing up to 100 % of EAFS with NA resulted in stiffer concrete, with greater compressive and flexural strength. After 28 days of curing, the compressive strength increased by 8.97 % and 30.90 % for the EAFS-50 and EAFS-100 series, respectively (Rojas et al., 2023).

Table 4.2: Average Compressive Strength of Concrete under Different
Concrete Categories.

	Concrete Categories						
	Control	**R1**	**R2**	**R3**	**15%**	**30%**	**45%**
Average Compressive Strength (MPa)	557.80	614.94	725.42	802.44	566.72	762.08	814.01
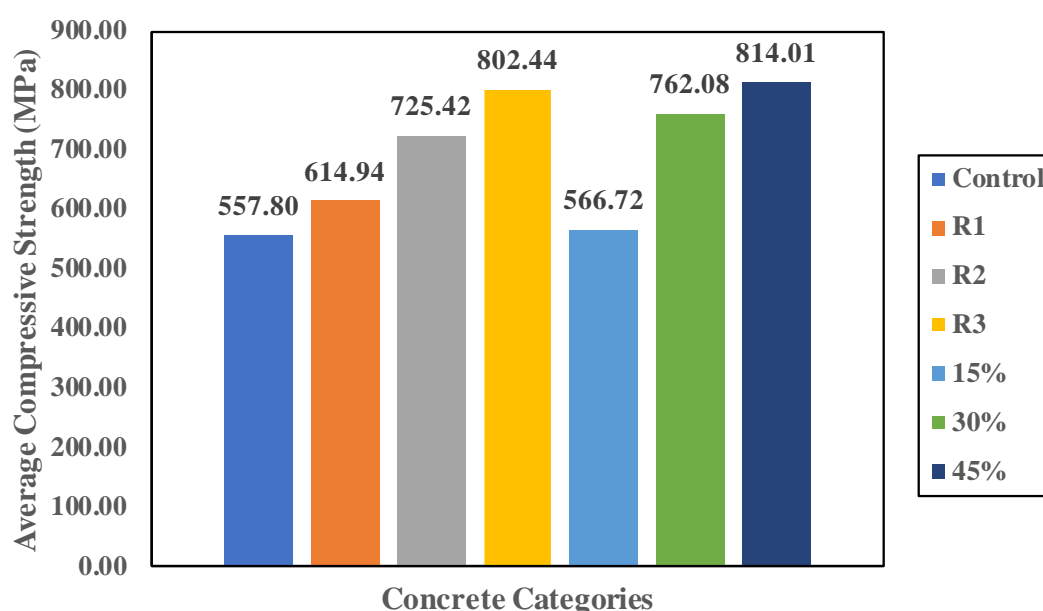
Figure 4.2: Average Compressive Strength of EAF Slag Concrete under
Different Concrete Categories.

4.2.2   Comparison with BOF Slag Concrete

Figure 4.3 is the bar chart constructed based on the results obtained from the average compressive strength of BOF slag concrete under different particle sizes and percentages of replacement. By referring to Figure 4.1 and Figure 4.3 below, it is found that the typical strength of concrete made with EAF slag and BOF slag varies depending on the replacement percentage (15 %, 30 % and 45 %) and particle size ranges (R1, R2 and R3). There are differences and similarities, between the two types of concrete. Generally, the average compressive strength of BOF slag concrete is limited to a range of 600 MPa to 850 MPa, showing a narrow range compared to EAF slag concrete which

ranges from 445 MPa to 880 MPa. EAF slag concrete also has a higher peak value of 879.90 MPa than BOF slag concrete which achieve average compressive strength of 843.23 MPa according to Table 4.3 below. In EAF slag concrete, the compressive strength usually increases with replacement percentages and larger particle sizes. For example, the average compressive strength at 45 % replacement is 684.50 MPa compared to 15 % replacement (445.80 MPa) in the R1 particle size range. This pattern is consistent across all particle size ranges (R1, R2 and R3) suggesting that increasing the EAF slag replacement percentage enhances strength. On the other hand, BOF slag concrete shows less uniformity in strength across different replacement percentages and particle size ranges. While some categories such as R2 45 % experience a strength increase with replacement percentages and larger particles, others exhibit fluctuations or even decreases in strength, for example, R3 45 %. Thus, while the results of the study enable the claim that EAF slag concrete could be stronger than BOF slag concrete, and the difference becomes more considerable with increasing extent of replacement and bigger particle size, additional research is necessary to reason the observed specifics of behaviour. They may concern the chemical contents of slags, properties of their particles, and concretes.

Table 4.3:   Average Compressive Strength of BOF Slag Concrete under
Different Particle Size Range and Percentage of Replacement.

Particle size Range	Average Compressive Strength (MPa)			
	Percentage of steel slag replacement (%)			
	0	15	30	45
R1	-	604.80	639.07	699.43
R2	-	775.13	770.60	788.40
R3	-	785.53	843.23	661.17
Control	557.80	-	-	-
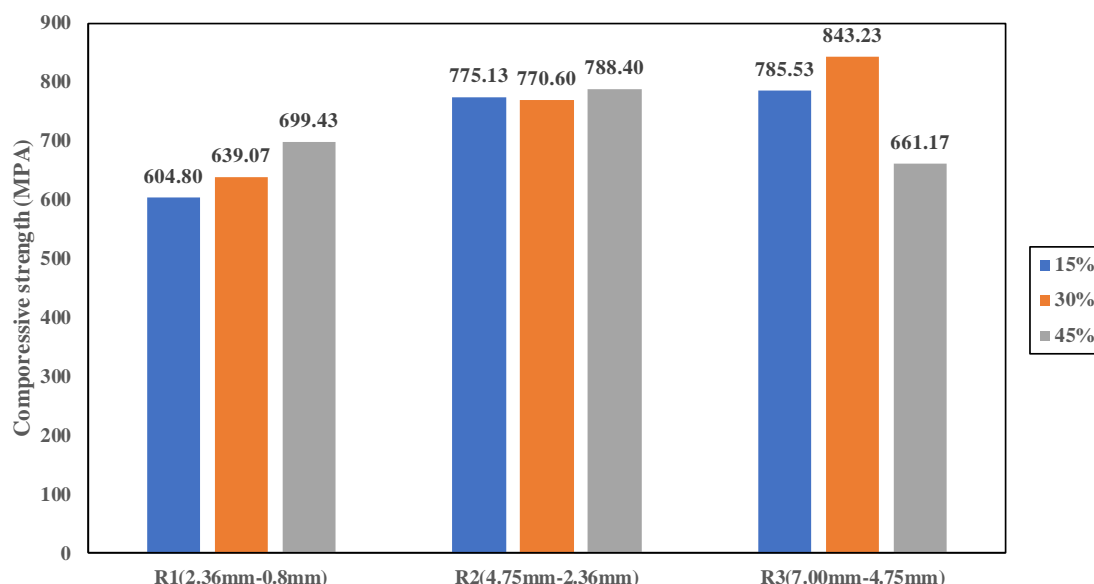
Figure 4.3: Average Compressive Strength of BOF Slag Concrete.

4.3 Energy Dispersive X-ray Spectroscopy (EDS) and Scanning Electron Microscopy (SEM)

4.3.1 EAF Slag

EDS is a useful test to detect almost all elements in the periodic table with only hydrogen and helium being the sole exceptions as they fail to emit the X-ray. EDS is always carried out along with SEM as combining SEM and EDS, enables scientists to understand the elemental composition of a specimen as well as its surface properties. EDS is also able to correlate the morphology of the sample with its chemical composition and provides valuable insight into the properties and behaviour of the sample. It allows targeted analysis and characterisation by identifying elements present in specific regions of interest within the sample. In this section, the elemental composition of control set concrete and EAF slag concrete from different particle size ranges, R1 (0.8 mm - 2.36 mm), R2 (2.36 mm – 4.75 mm), and R3 (4.75 mm - 7 mm) are summarized in Table 4.4 in term of percentage (At%) to help to identify the optimum particle size of EAF slag for carbon capture.

Table 4.4: Elemental Composition of EAF Slag Concrete Samples with
Different Particle Size Range and Percentage of Replacement.

Sample	Percentage (%)	Element (At%)					
		Ca, Calcium	Mg, Magnesium	O, Oxygen	Al, Aluminium	Si, Silica	C, Carbon
	15	65.13	2.53	12.14	4.12	14.92	0.94
R1	30	58.06	0.96	15.42	1.76	22.88	0.92
	45	76.64	0.97	10.31	1.56	9.44	1.08
	15	63.42	3.16	16.91	2.2	12.77	1.54
R2	30	66.04	3.07	18.08	3.07	12.04	2.61
	45	82.2	0.94	6.74	1.11	8.46	0.54
	15	82.04	7.84	7.29	1.13	7.84	0.65
R3	30	67.77	2.21	13.47	2.11	13.41	1.03
	45	68.7	1.58	14.31	2.42	10.63	1.37
Control	100	56.21	1.41	19.19	4.21	17.5	1.48

The elements calcium (Ca), silicon (Si), magnesium (Mg), and carbon (C) are the focus of this study. These elements are involved in carbon sequestration by converting carbon dioxide into new chemical compounds, as well as being the main contributors to the compressive strength of concrete. In carbon capture processes, for example, carbon (C) is the primary element captured. This involves the capture of carbon dioxide (CO_2) emissions from industrial processes or the generation of electricity before they are released into the atmosphere. In some carbon capture technologies, materials containing silicon, such as silicates, are used to chemically absorb the CO_2 from the flue gas. Calcium (Ca) reacts with CO_2 to form stable carbonates and is also present in cementitious materials such as Portland cement; calcium compounds hydrate during the curing process to form calcium silicate hydrate (C-S-H) gel, which contributes to concrete strength. Magnesium (Mg) is

similar to calcium; magnesium-based sorbents can be used in carbon capture processes to chemically absorb CO_2 and form stable carbonates. By referring to Figure 4.4 which shows the bar chart of the elemental composition of concrete samples under different categories, there are noticeable patterns in the study of the elemental composition of EAF slag concrete and its effect on carbon storage and compressive strength. In terms of calcium content, it's observed that concrete of R2 at a 45 % EAF slag replacement level has the highest concentration, in contrast to the control set which has the lowest calcium content. This increased presence of calcium plays a key role in promoting the strength development of EAF slag concrete, culminating in higher compressive strength compared to conventional concrete. Moreover, steel slag has a promising potential for carbon dioxide reaction due to its high calcium content, this capability has recently been exploited in mineral carbonation processes, where steel slag serves as the primary material for carbon dioxide sequestration and carbon emission reduction (Mehrdad Mahoutian et al., 2014). When considering the silicon content, concrete of R1 with 30 % EAF slag replacement has the highest silicon content at 22.88 %, while R3 with 15 % replacement has the lowest at only 7.84 %. This variation in silicon content highlights the different structural characteristics and performance potential of different EAF slag concrete formulations. The analysis of the magnesium content shows that the highest magnesium content of 7.84 % is found in R3, while the lowest magnesium content of 0.94 % is found in R2. This discrepancy highlights the influence of magnesium on the properties of the material and suggests a possible impact on the structural integrity and durability of the material. In terms of carbon, concrete of R2 at the 30 % EAF slag replacement level has the highest carbon content at 2.61 %, whereas concrete of R2 at the 45 % EAF slag replacement level has the lowest carbon content at 0.54 %. This variance in carbon content can have a significant impact on the carbon sequestration capacity of the material, potentially affecting its environmental sustainability profile.
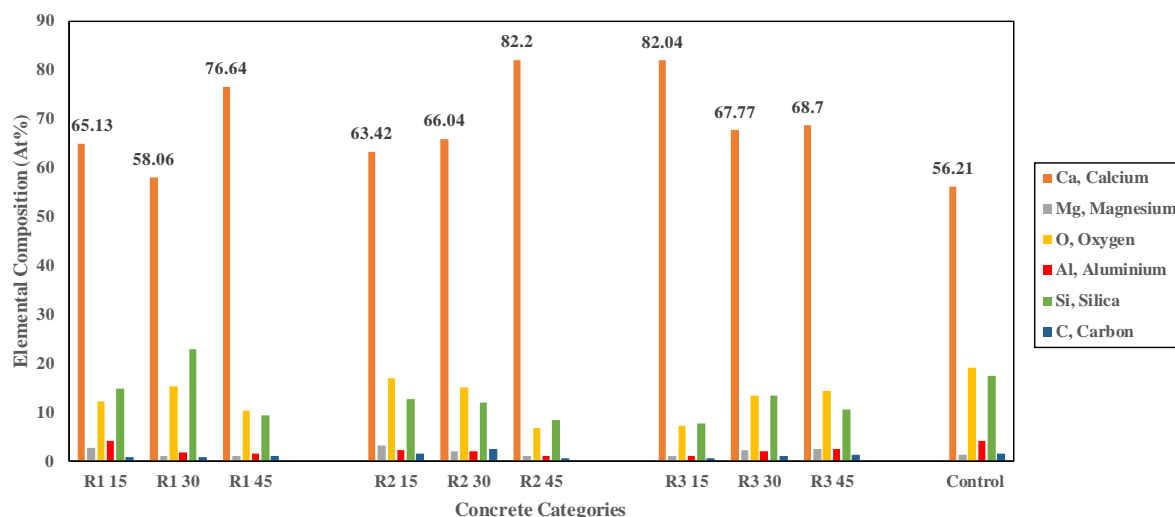
Figure 4.4: Elemental Composition of EAF Concrete Samples under Different Concrete Categories.

The other area that can be explored will be the replacement rate of EAF slag of the concrete. Figure 4.4 above illustrates that the concrete containing R1 EAF slag at a replacement level of 15 %, has a favourable elemental composition which is better than samples that contain R2 or R3 slag. Among the three particle size groups, R1 exhibits the highest calcium content, the highest aluminium, and the highest silica content. Remarkably, the R1 group has the smallest carbon content, even when compared to the control group. The findings indicate that applying R1 concrete can improve mechanical properties and maintain durability without any significant deviation from the control mix. When the replacement level is increased to 30 %, R2 EAF slag concrete presents an overall higher elemental composition when compared with particles in other size ranges, but with a lesser amount of calcium content. It should be mentioned that R2 has the highest carbon content percentage, which is around 2.61 %. This indicates, among other things, the possible effects on carbon capture and strength of the R2 concrete mix. Concrete added with R3 EAF slag at a 45 % replacement level demonstrates a higher overall elemental composition when compared to the other particle size ranges. Nevertheless, it is the one with the least calcium from these three. However, R3's underlying asset allocation is still fairly diversified. The result is most probably that it will improve both the present performance and

subsequent endurance of the concrete. Nevertheless, the concern about calcium availability should not be overlooked.

On the other hand, SEM analysis is conducted on the normal concrete (control set) and EAF slag concretes of R1 15 %, R2 30 %, and R3 45 % mentioned to study the morphology of the respective concrete under a magnification of 2000 ×. The SEM pictures of these concrete samples, which are shown in Figures 4.5 and 4.6 below, have text and red circles annotated on them to help identify the surface morphology and label the different compounds and structural elements that are present in the concrete samples.
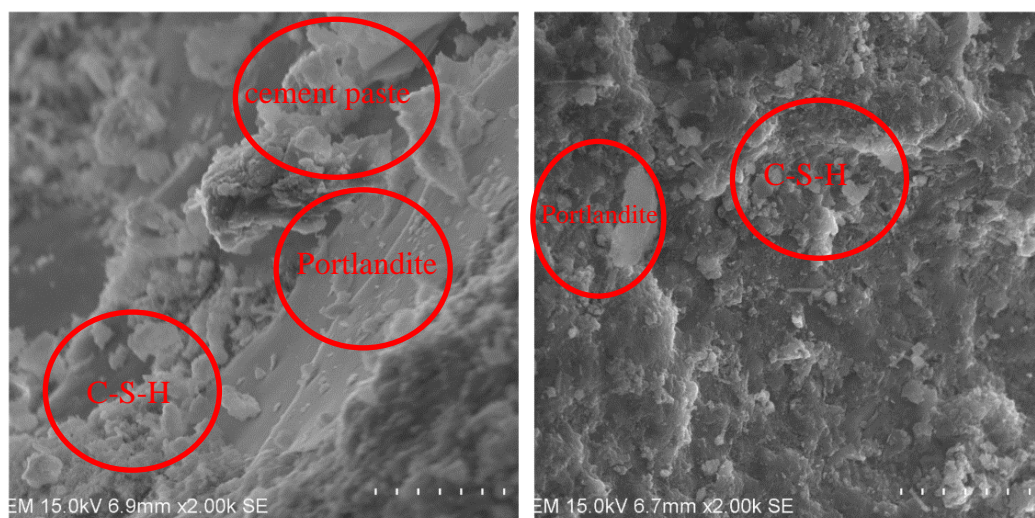

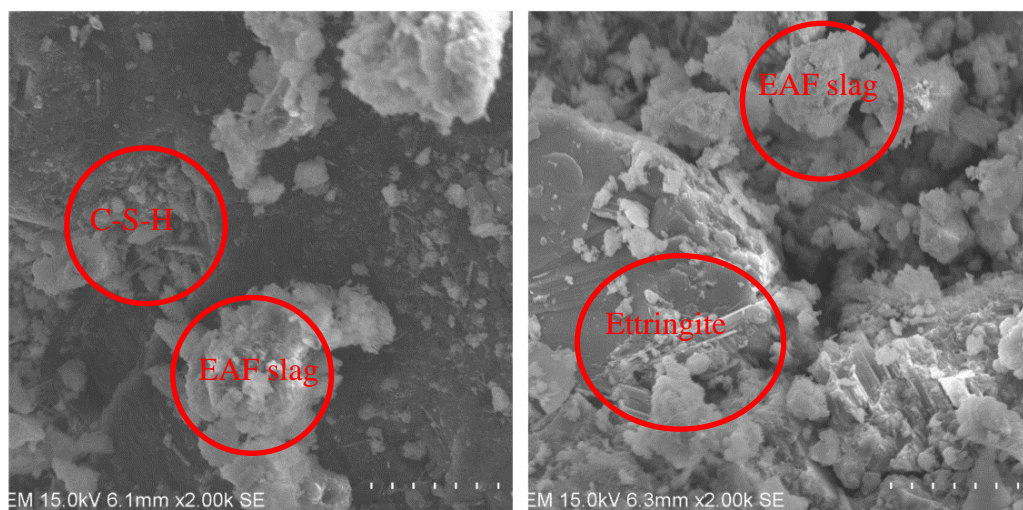Figure 4.5: (Left) SEM of control set. (Right) SEM of R1 15%.

Figure 4.6: (Left) SEM of R2 30 %. (Right) SEM of R3 45 %.

4.3.2   Comparison with BOF Slag

Table 4.5 is constructed to summarise the elemental composition of BOF slag concrete samples with different particle size ranges and percentages of replacement. Meanwhile, Figure 4.7 which shows a bar chart that visualises the elemental composition of BOF slag concrete also added below. After reviewing the tables (Table 4.4 and Table 4.5) and graphs (Figure 4.6 and Figure 4.7) below, it is noticed that the elemental composition of EAF slag concrete and BOF slag concrete are different. Generally, EAF slag concrete has a higher percentage of calcium (Ca) within a range of 58.06 % to 82.20 % while the percentage of Ca in BOF slag is only within the range of 20.57 % to 25.27 %. Similar to EAF slag concrete, the highest calcium percentage falls within the R2 particle size range, with a difference in replacement rate of 45 % in EAF slag and 30 % in BOF slag. The low calcium content in BOF slag concrete may result in a lower compressive strength and lower carbon capture ability as calcium is one of the main elements for the formation of calcium carbonate in the process of carbonation to capture the carbon dioxide from the atmosphere. On the other side, BOF has a high and stable percentage of oxygen elements (53.96 % - 61.93 %) among all the nine categories and the highest value (61.93 %) falls within the R1 15 % category. Besides, the carbon element in BOF slag concrete is generally higher than in EAF slag concrete, this may help BOF slag concrete to have good carbon capture ability, but the percentage of carbon element varies and is not as consistent as EAF slag concrete. In this case, R3 45 % poses the highest percentage of carbon elements which is 15.74 % among all the categories of BOF slag concrete. The magnesium, aluminium and silica element composition of both EAF slag concrete and BOF slag concrete are similar and consistent. However, the percentage of magnesium (1.15 % - 1.78 %), aluminium (1.19 % - 2.06 %), and silica elements (5.11 % - 8.22 %) of BOF slag are generally lower than EAF slag concrete. From previous discussion, it can be found that the effect of these elements on the carbon capture ability of steel slag is favourable, and hence it is suggested that EAF slag has better carbon capture ability than BOF slag.

Table 4.5: Elemental Composition of BOF Slag Concrete Samples with
Different Particle Size Range and Percentage of Replacement.

| Sample	Percentage (%)	Element (At%)					
		Ca, Calcium	Mg, Magnesium	O, Oxygen	Al, Aluminium	Si, Silica	C, Carbon
	15	22.45	1.72	57.68	1.89	5.11	11.15
R1	**30**	25.17	1.73	55.94	2.06	6.49	8.61
	45	20.57	1.66	61.93	1.73	5.71	8.40
	15	21.54	1.15	59.74	1.19	5.68	10.07
R2	**30**	25.27	1.5	57.23	1.85	6.49	7.66
	45	22.48	1.27	56.65	1.65	6.38	8.01
	15	22.59	1.58	53.96	2.03	7.22	15.74
R3	**30**	23.00	1.6	56.57	1.63	8.22	7.1
	45	23.27	1.78	57.4	1.82	6.04	9.69
Control	**100**	56.21	1.41	19.19	4.21	17.5	1.48
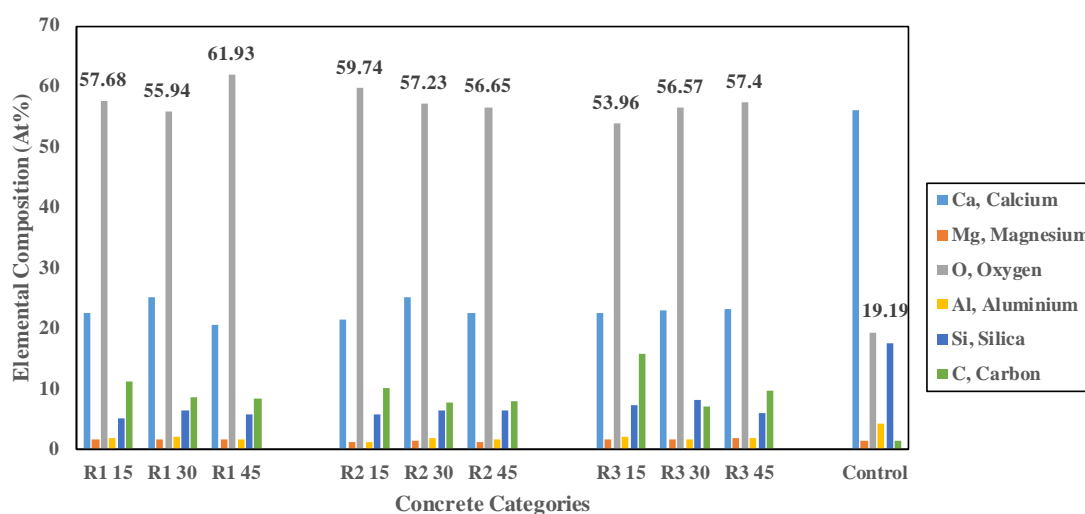
Figure 4.7: Elemental Composition of BOF Concrete Samples under Different
Concrete Categories.

4.4 X-ray Diffraction (XRD)

4.4.1 EAF Slag

X-ray diffraction is another analytical technique that is commonly used for studying the crystallinity of materials using X-rays. X-ray examination is performed by packing the sample with a stream of X-rays. A diffraction pattern of the sample is then seen, and the interpretation value provides information on how the atoms are organized or packed within the material. X-ray diffraction is used for the identification of the crystals of compounds, the measurement of their purity, and research on phase changes or structural conversion in a variety of environmental conditions. Furthermore, it's applied to investigate bonding between atoms and visualise the existence of impurities or deficiencies, with high precision study nanomaterials of remarkable importance. In this study, the setting of X-ray diffraction (XRD) follows the setup of using a gonio scan axis which is configured with specific parameters to ensure accurate data collection. The scan range is set and fixed at a range of $5.0000°$ to $85.0000°$ 2θ, with a fine step size of $0.0200°$ 2θ. The scan step time is set as 1.0000 seconds and a $0.0000°$ 2θ offset is maintained for alignment accuracy. Meanwhile, the utilisation of a pre-set time scan type ensures consistency of data acquisition across samples. Beam divergence during measurements is controlled using the fixed divergence slit type with a size of $1.0000°$. The sample length is limited to 10.00 mm with a receiving slit size of 0.1000 mm to optimise the detection of diffracted X-rays. Operation at a stable measurement temperature of 25.00 °C ensures reproducibility in experiments. The XRD system utilises a Cu anode material with characteristic wavelengths of K-Alpha1 at 1.54060 Å and K-Alpha2 at 1.54443 Å, which provides essential information for accurate data analysis. Meanwhile, Figure 4.8 shows the XRD graph of the R3 45 % concrete sample and its chemical composition by using X-pert HighScore Plus software as the analysis tool.
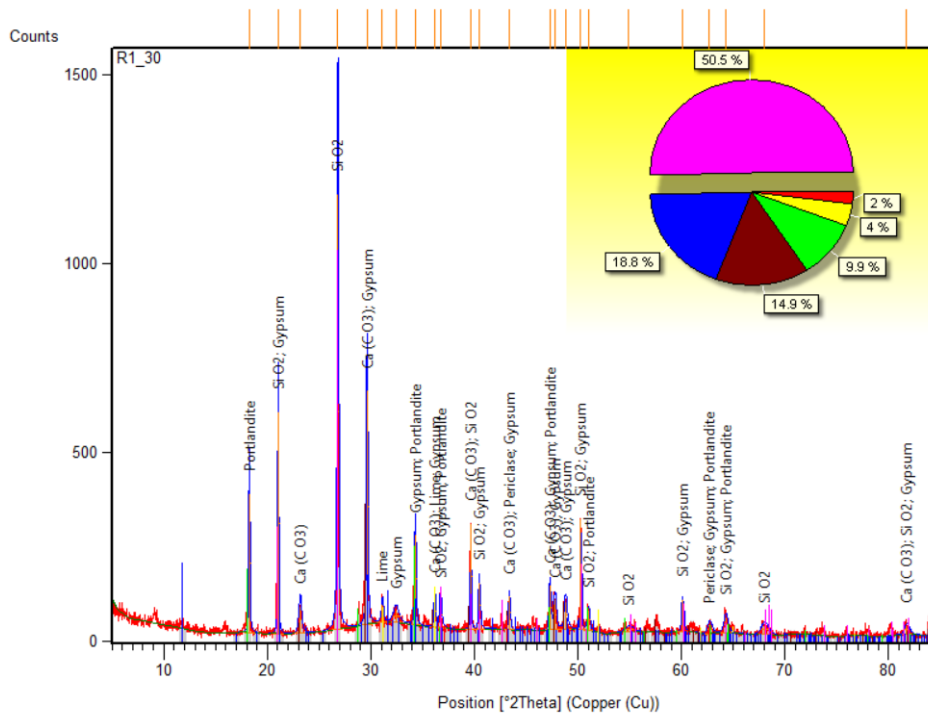
Figure 4.8: XRD Graph of R1 30 % Concrete Sample.

By referring to the XRD graph (Figure 4.8) above, the results show that the pattern list of R1 30 % concrete sample matches with several chemical compounds from the Crystallography Open Database. The compounds found in the R1 30 % concrete sample include periclase (MgO), calcium carbonate ($CaCO_3$), portlandite (Ca $(OH)_2$), silicon dioxide (SiO_2), gypsum ($CaSO_4.2H_2O$), and lime (CaO). Using X-pert HighScore Plus simplifies the identification of these chemical compounds and provides information about their relative composition. As an illustration, the composition chart positioned in the top right corner displays various colours, each representing a specific chemical compound. The dark red colour signifies calcium carbonate, with a relative weightage of 14.9 %, while the pink colour indicates that the percentage of silicon dioxide is 50.5 % as depicted in Figure 4.8. This process facilitates the systematic and accurate collection of data. After carrying out XRD analysis on normal concrete and EAF slag concretes the chemical compounds of the concretes are summarised in Table 4.6 below.

Table 4.6:   Chemical Compounds of EAF Slag Concretes.

Concrete	Chemical Compound (wt.%)							
	CaO	SO$_3$	MgO	CaCO$_3$	SiO$_2$	Portlandite	Gypsum	C
Control	5	0	13	33	37.6	12.9	24.8	0
R1 15%	3	0	9	67	6	14	0	0
R1 30%	5.1	0	5.1	28.3	50.5	9.9	18.8	0
R1 45%	5	0	15	26	30	0	43	0
R2 15%	3	0	4	59.6	58.4	7.9	0	0
R2 30%	4	0	8.9	55.4	3	17.8	0	17.8
R2 45%	9.1	0	32.3	28.3	46	14	24	0
R3 15%	3	0	5	56	29	17	0	0
R3 30%	4	0	7	27	67	7	13	0
R3 45%	4	0	11.9	51.5	14.9	12.9	17.8	0

According to Abu-Eishah, El-Dieb and Bedir's (2012) findings, EAF steel slag typically consists of CaO, SiO$_2$ and ferrous oxide (FeO) roughly in the percentage of 40 %, 17 %, and 20 % respectively. Other oxides such as aluminium oxide (Al$_2$O$_3$), MgO and manganese (II) oxide (MnO) are also present in concentrations ranging from 0.4 % to 10 %. Yildirim and Prezzi (2011) suggest that EAF slags typically contain 10 - 40 % FeO, 22 - 60 % CaO, 6 - 34 % SiO$_2$, 3 - 14 % Al$_2$O$_3$ and 3 - 13 % MgO respectively. However, the chemical composition of EAF slag concrete shows a significant presence of CaO, MgO, and SiO$_2$ but with varying levels of SO$_3$, gypsum, quartz, portlandite and carbon between different concrete samples. The XRD results differ slightly from previous research, with only CaO, MgO and SiO$_2$ being detected, while FeO, Al$_2$O$_3$, and MnO are conspicuously absent. There are also differences in the percentage composition. However, this variation can be attributed to the analysis of concrete samples containing EAF slag rather than pure EAF slag. The absence of specific compounds in the concrete samples could be attributed to inherent differences between EAF slag concrete samples and their pure EAF slag counterparts. The scarcity of samples is suggested to be another factor that results in varying levels of chemical compounds in each concrete. In the XRD test, only one sample from each concrete category is sent

for analysis. This results in a lack of comparative data among each category and leads to less consistent results.

The chemical compounds of control set concrete and EAF slag concrete that identified by XRD analysis included calcium oxide (CaO), sulphur trioxide (SO_3), magnesium oxide (MgO), silicon dioxide (SiO_2), portlandite (Ca $(OH)_2$), gypsum ($CaSO_4.2H_2O$), calcium carbonate ($CaCO_3$), and carbon (C). In fact, CaO is a key component in EAF slag concrete that contributes to its carbon capture capacity. During the carbonation process, calcium oxide (CaO) reacts with carbon dioxide (CO_2) from the atmosphere to form calcium carbonate ($CaCO_3$), effectively sequestering CO_2 within the concrete matrix. A higher CaO content generally indicates a greater potential for carbon capture. Although SO_3 is not directly involved in carbon capture reactions, its presence can influence the properties of the concrete. Excessive sulphur content can lead to the formation of calcium sulphate ($CaSO_4$), which may affect the reactivity of CaO with CO_2 and potentially reduce carbon capture capacity. Although MgO can also participate in carbonation reactions, its contribution is lesser compared to CaO. Its presence enhances carbonation kinetics and carbon capture capacity by contributing to the overall alkalinity of the concrete. The chemical compounds discussed above play an important role in affecting the carbon capture capacity of concrete as the maximum theoretical CO_2 uptake can be calculated by using the weightage of these chemical compounds such as lime, periclase, sulphur trioxide, calcium carbonate, dipotassium oxide, and disodium oxide. After obtaining the weightage data, the maximum theoretical CO_2 uptake is calculated using equation 4.1 and simplified equation 4.2, Stenoir's stoichiometric equation, as described by Omale et al (2019). Since dipotassium oxide and disodium oxide are not found in XRD analysis, equation 4.2 will be used to calculate the maximum theoretical CO_2 uptake. The results are summarised in Table 4.7 and presented as a clustered bar chart in Figure 4.9 below.

$$\%CO_2 = 0.785(\%CaO - 0.56\,\%CaCO_3 - 0.7\,\%SO_3)$$
$$+1.091\,\%MgO + 0.71\,\%Na_2O + 0.468\,\%K_2O \qquad (4.1)$$

$$\%CO_2 = 0.785(\%CaO - 0.7\,\%SO_3) + 1.091\,\%MgO \qquad (4.2)$$

Table 4.7: Maximum CO_2 Uptake of Concrete.

Concrete	Maximum CO_2 Uptake (%)
Control	9.10
R1 15 %	12.17
R1 30 %	5.32
R1 45 %	12.17
R2 15 %	2.97
R2 30 %	11.76
R2 45 %	18.41
R3 15 %	6.72
R3 30 %	5.32
R3 45 %	6.41
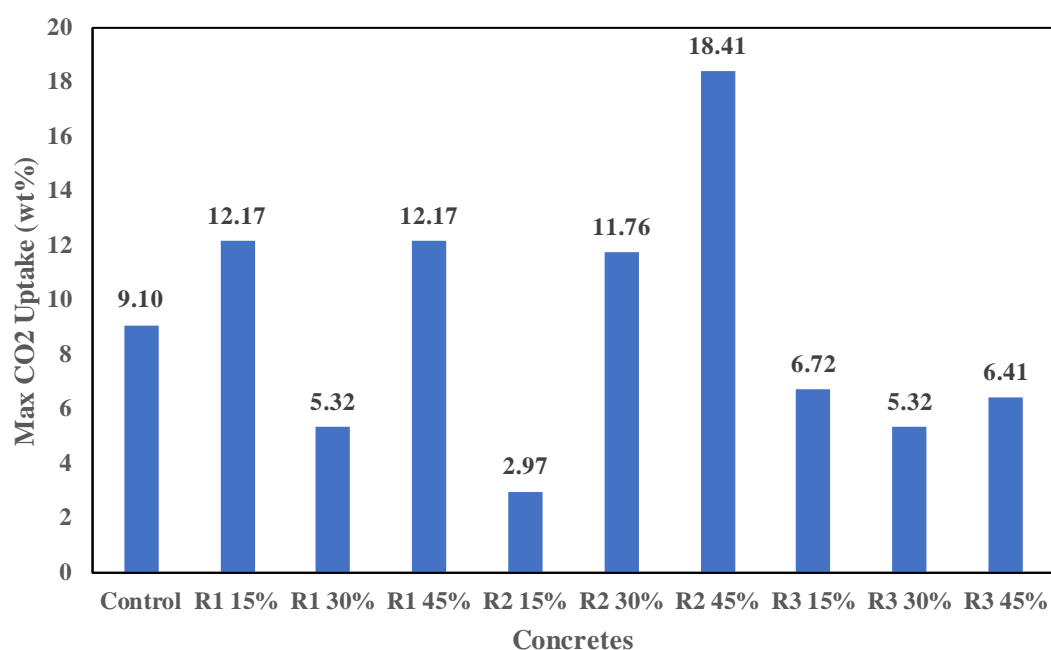
Figure 4.9: Maximum CO_2 Uptake of Various Concretes.

Figure 4.9 shows that the maximum CO_2 uptake value for normal concrete (control) is 9.10 %. Among the EAF concrete mixes, R2 with 45 % EAF slag content has the highest maximum CO_2 uptake value at 18.41 %. This is followed by R1 45 % and R1 15% EAF slag content at 12.17 % and R2 with 30 % EAF slag content at 11.76 %. Among all the mixes tested, R2 with 45 % EAF slag content concrete exhibits the highest carbon capture capacity. The data overall suggests that incorporating higher percentages of EAF slag into concrete mixes enhances their carbon capture capacity. The results obtained show better performance compared with previous studies which have shown that steel slag can capture up to 5.836 wt. % (58.36 g CO_2/kg of steel slag) of

its theoretical carbon sequestration capacity based on its mass (Omale et al, 2019). This is probably because of the presence of calcium oxide (CaO) in EAF slag, which can react with atmospheric CO_2 during the curing process to form calcium carbonate ($CaCO_3$), effectively sequestering carbon dioxide within the concrete matrix. As a result, EAF concrete shows promise as a sustainable building material with the potential to reduce carbon emissions through carbon capture and utilisation.

On the other hand, the high levels of calcium carbonate ranging from 26 % to 67 % found in EAF concrete as shown in Table 4.6 may result from multiple reasons. The reason behind this may be associated with a direct reaction between calcium ions and carbon dioxide (CO_2) during the hardening of the concrete elements. Furthermore, it is possible that materials that are rich in calcium carbonate are being added to the concrete mixture during the concrete casting process. The level of $CaCO_3$ concentration in concrete significantly increases the amount of CO_2 being captured. Calcium carbonate is created when ambient CO_2 enters concrete pores and combines with the calcium hydroxide (Ca $(OH)_2$) that is produced during the cement hydration process. In the form of calcium carbonate, this process efficiently sequesters CO_2 within the concrete matrix. Hence, a cement with a higher concentration of CaCO3 traps more CO_2, as it facilitates more sites to absorb the gas. Additionally, having high levels of silicon dioxide (3 % - 67 %) will also help to raise the alkalinity of the concrete. The highly alkaline environment resulting from silicon dioxide improves the formation of calcium carbonate and sequesters carbon dioxide through carbonation. Furthermore, the hydration reaction between Portland cement also releases another chemical known as portlandite or calcium hydroxide (Ca $(OH)_2$) when calcium oxide (CaO) from cement reacts with water. Portlandite does not actively participate in the strength of concrete under compression, but it can facilitate this process. Through the process of carbonation, carbon dioxide is effectively captured and completely sequestered, keeping it out of the atmosphere. This can help mitigate global warming by decarbonizing concrete production while also making concrete more sustainable.

Therefore, calcium carbonate ($CaCO_3$), silicon dioxide (SiO_2), and portlandite also have the potential for carbon capture within the concrete matrix. $CaCO_3$ can be formed directly by the carbonation of CaO, portlandite can react with carbon dioxide from the atmosphere that penetrates concrete to form calcium carbonate, while carbon or CO_2 can be sequestered by mineral carbonation reactions involving CaO and other reactive compounds in the concrete mix. The presence of these chemical compounds is beneficial for the long-term sustainability of concrete in terms of carbon capture potential.

4.4.2   Comparison with BOF Slag

Table 4.8 shows the chemical compounds of BOF slag concrete, and these results will be used for discussion and comparison with EAF slag concrete to understand and study their difference in terms of carbon capture ability. By making a comparison between the chemical compositions of EAF slag concrete and BOF slag concrete, the first difference that was found is the difference in the number and type of chemical compounds. The number of chemical compounds found in EAF slag concrete is higher than in BOF slag and shows variation in the type of chemical constituent. Eight types of chemical compounds with varying levels were found and studied for EAF slag concrete in the previous discussion. However, BOF slag concrete shows a fixed chemical constituent consisting of six types of chemical compounds which are calcium carbonate, carbon, periclase, silicon dioxide, lime, and portlandite. In EAF slag concrete, the dominant compounds include gypsum, calcium carbonate, and silicon dioxide, with variations observed across different replacement levels. Besides, EAF slag concrete exhibits higher percentages of lime and periclase than BOF slag concrete. In the opposition, BOF slag has higher carbon content indicating a different chemical composition. EAF slag concrete generally displays lower carbon content but higher levels of calcium carbonate and lime, suggesting a potential advantage in terms of carbon capture potential due to the presence of calcium-based compounds. For instance, the peak calcium carbonate and calcium oxide content in EAF slag concrete is observed in R1 15 % and R2 45 %, reaching up to 67 % and 9.10 % respectively. On the other hand, BOF slag concrete only peaks at 50 % in R2 45 % and R3 15 % for calcium carbonate and peaks

at 5 % at R1 30 % for lime. Nevertheless, it is notable that the lowest recorded carbon content in EAF slag concrete is 0 %, while BOF slag concrete registers a minimum of 1 %. Next, the silicon dioxide of BOF slag concrete is generally higher with peak value of 73.7 % in R3 30 % than EAF slag concrete which poses 67 % of silicon dioxide in R3 30 %. These variances underscore the complex interplay between elemental composition and carbon capture potential, emphasizing the need for comprehensive analysis when selecting between EAF and BOF slag concrete for environmentally sustainable construction applications.

Table 4.8: Chemical Compounds of BOF Slag Concretes.

Concrete	Chemical Compound (wt.%)					
	CaCO$_3$	Carbon	Periclase	SiO$_2$	Lime	Portlandite
R1 15%	23	2	1	68	3	3
R1 30%	16	15	10	34	5	20
R1 45%	29	8	6	36	3	18
R2 15%	11.1	46.5	10.1	24.2	1	7.1
R2 30%	10.2	23.5	2	49	2	13.3
R2 45%	50	7	3	32	2	6
R3 15%	50	12	4	23	2	9
R3 30%	13.1	3	2	73.7	1	7.1
R3 45%	15.8	34.7	2	36.6	1	9.9
Control	33	9	9	30	5	14

4.5   Summary

The previous results and discussion highlight the better performance of EAF slag concrete when comparing to both conventional concrete and BOF slag concrete across tests and analysis such as compression test, XRD, SEM and EDS.

In the compression test, it was observed that EAF slag concrete presented higher compressive strength values than conventional concrete and BOF slag concrete. Especially, the peak compressive strength reached 879.90 MPa for R3 45% EAF slag concrete, surpassing the peak value of 843.23 MPa observed in BOF slag concrete.

In the EDS test, the analysis discovered that EAF slag concrete contained higher levels of calcium and silica compared to BOF slag concrete. Specifically, the highest percentages of calcium and carbon were observed within the particle size range R2. Additionally, EAF slag concrete exhibited elevated levels of calcium, aluminium, magnesium, and silica but lower levels of oxygen and carbon compared to BOF slag concrete. SEM of control set, R1 15 %, R2 30 %, and R3 45 % also conducted to explore the surface morphology, the different compounds, and structural elements that are present in the concrete samples.

In XRD test, the analysis identified various chemical compounds present in EAF slag. This included the calcium oxide, sulphur trioxide, magnesium oxide, silicon dioxide, portlandite, gypsum, calcium carbonate, and carbon. By using Stenoir's stoichiometric equation, it was determined that EAF slag concrete possesses significant carbon capture capacity. Besides, the maximum CO_2 uptake capacity was calculated, with the highest value of 18.41 % achieved by EAF slag concrete (R2 45 %). This ability to capture carbon dioxide is due to the presence of calcium carbonate, silica, and portlandite in EAF slag concrete, which enhance its carbon capture capabilities.

Overall, the results show that EAF slag concrete demonstrates superior mechanical strength, chemical composition, and carbon capture potential compared to conventional and BOF slag concrete, offering promising prospects for sustainable construction materials.

CHAPTER 5

CONCLUSIONS AND RECOMMENDATIONS

5.1 Conclusions

In conclusion, this study demonstrated the potential of electric arc furnace (EAF) slag as one of the carbon capture materials, and its positive effect on enhancing the compressive strength of concrete. This study's aim focuses on assessing the effectiveness of EAF slag in carbon capture capacity and exploring the performance of EAF slag concrete with conventional concrete.

The first objective of this study is to find out the optimum particle size range of EAF slag for carbon capture. After a series of experiments and analyses, it was concluded that the optimum particle size range of EAF slag for CO_2 capture was 4.75 mm to 2.36 mm, which was in the R2 particle size range. This is corroborated by the elemental analyses using Energy Dispersive X-ray Spectroscopy (EDS) testing which show that the concrete samples containing EAF slag had high carbon content (2.61%) and high calcium content (82.2%), with the highest values within R2 particle size range. This shows the revolutionary ability of concrete structures fabricated from EAF slag to both slow down climate change and provide better structural strength.

The second objective of this study is to evaluate the carbon capture capacity of EAF slag. By using Stenoir's stoichiometric equation, the maximum theoretical carbon uptake capacity of EAF slag concrete is calculated. Among the results, EAF slag concretes show higher carbon capture capacity than control set concrete at a 45 % replacement rate. R2 EAF slag concrete also yields the highest carbon capture capacity of 18.41 % theoretically based on Stenoir's stoichiometric equation.

The third objective of this study is to compare the compressive strength of EAF slag concrete and conventional concrete. After conducting a compression test, there was no denying the superiority of EAF slag concrete over conventional concrete in terms of compressive strength, with the former having a higher average compressive strength overall and a peak compressive strength of 879.90 MPa recorded in the R3 particle size range.

Thus, the aim and objectives of the study were essentially met, and these particular result values highlight the significant benefits of incorporating the potential of EAF slag waste streams into the carbon capture processes and their application in concrete production. These results provide a strong path forward for mitigating environmental impact and a concrete chance for the construction sector to adopt sustainable innovations, contributing to a more resilient and environmentally friendly built environment for future generations.

5.2   Recommendations for future work

The main focus of this study is on the carbon capture potential of EAF slag, and the compressive strength comparison between EAF slag concrete and conventional concrete. However, the other engineering properties of EAF slag concrete such as flexural strength, durability, porosity, and others are not under study. Variables that might influence its ability to capture carbon were not considered as well. So, here are some of the recommendations for future work:

(i)   Study the effect of temperature fluctuations on carbon capture performance of EAF slag. The stability and efficiency of EAF under different operating conditions can be observed by evaluating its performance at various temperatures.

(ii)   Analyse the influence of moisture content on affecting the carbon capture capacity of EAF slag. This is crucial to understanding how moisture levels affect the performance of EAF slag to absorb and retain CO_2.

(iii)   Assess the durability of captured carbon in EAF slag in the long term to determine its suitability for carbon capture and storage applications. The long-term stability assessment of EAF slag is important in guaranteeing the feasibility and efficiency of utilising EAF slag as carbon capture materials.

REFERENCES

Abu-Eishah, S.I., El-Dieb, A.S. and Bedir, M.S., 2012. Performance of concrete mixtures made with electric arc furnace (EAF) steel slag aggregate produced in the Arabian Gulf region. *Construction and Building Materials*, [e-journal] 34, pp.249–256. https://doi.org/10.1016/j.conbuildmat.2012.02.012.

Akhtar, K., Khan, S.A., Khan, S.B. and Asiri, A.M.， 2018. Scanning Electron Microscopy: Principle and Applications in Nanomaterials Characterization. *Handbook of Materials Characterization*, [e-journal] pp.113–145. https://doi.org/10.1007/978-3-319-92955-2_4.

Ali, A., Chiang, Y.W. and Santos, R.M.， 2022. X-ray Diffraction Techniques for Mineral Characterization: A Review for Engineers of the Fundamentals, Applications, and Research Directions. *Minerals*, [e-journal] 12(2), p.205. https://doi.org/10.3390/min12020205.

Bodor, M., Santos, R., Gerven, T. and Vlad, M.，2013. Recent developments and perspectives on the treatment of industrial wastes by mineral carbonation — a review. *Open Engineering*, [e-journal] 3(4). https://doi.org/10.2478/s13531-013-0115-8.

Bunaciu, A.A., Udriştioiu, E. gabriela and Aboul-Enein, H.Y.， 2015. X-Ray Diffraction: Instrumentation and Applications. *Critical Reviews in Analytical Chemistry*, 45(4), pp.289–299. https://doi.org/10.1080/10408347.2014.949616.

Chandini, R.， 2017. Use of Steel Slag in Concrete as Fine Aggregate. *International Journal of Engineering and Innovative Technology (IJEIT)*, [e-journal] Volume 7(Issue 4). https://doi.org/10.17605/OSF.IO/EFGPN.

Escalante, J., Chen, W.-H., Tabatabaei, M., Hoang, A.T., Kwon, E.E., Andrew Lin, K.-Y. and Saravanakumar, A.， 2022. Pyrolysis of lignocellulosic, algal, plastic, and other biomass wastes for biofuel production and circular bioeconomy: A review of thermogravimetric analysis (TGA) approach. *Renewable and Sustainable Energy Reviews*, [e-journal] 169(112914), p.112914. https://doi.org/10.1016/j.rser.2022.112914.

Felix, C.B., Chen, W., Ubando, A.T., Park, Y.-K., Kun-Yi Andrew Lin, Arivalagan Pugazhendh, Nguyen, T.N. and Dong, C.， 2022. A comprehensive review of thermogravimetric analysis in lignocellulosic and algal biomass gasification. *Chemical Engineering Journal*, [e-journal] 445(136730), pp.136730–136730. https://doi.org/10.1016/j.cej.2022.136730.

Fewster, P.F.， 2023. The Limits of X-ray Diffraction Theory. *Crystals*, [e-journal] 13(3), pp.521–521. https://doi.org/10.3390/cryst13030521.

Grace, J.， 2013. Carbon Cycle. *Encyclopedia of Biodiversity*, [e-journal] pp.674–684. https://doi.org/10.1016/b978-0-12-384719-5.00306-3.

Haug, T.A., Kleiv, R.A. and Munz, I.A.，2010. Investigating dissolution of mechanically activated olivine for carbonation purposes. *Applied Geochemistry*, [e-journal] 25(10), pp.1547–1563. https://doi.org/10.1016/j.apgeochem.2010.08.005.

Hodoroaba, V.-D., 2020. Energy-dispersive X-ray spectroscopy (EDS). *Characterization of Nanoparticles*, [e-journal] pp.397–417. https://doi.org/10.1016/b978-0-12-814182-3.00021-3.

Larachi, F., Daldoul, I. and Beaudoin, G., 2010. Fixation of CO2 by chrysotile in low-pressure dry and moist carbonation: Ex-situ and in-situ characterizations. *Geochimica et Cosmochimica Acta*, [e-journal] 74(11), pp.3051–3075. https://doi.org/10.1016/j.gca.2010.03.007.

Mohammed, A. and Avin Abdullah., 2019. Scanning Electron Microscopy (SEM): A Review. [online] Available at:<https://www.researchgate.net/publication/330168803_Scanning_Electron_Microscopy_SEM_A_Review.> [Accessed 17 August 2023].

None Akhil and Singh, N., 2023. Microstructural characteristics of iron-steel slag concrete: A brief review. *Materials Today: Proceedings*, [e-journal] https://doi.org/10.1016/j.matpr.2023.03.548.

Omale, S.O., Choong, T.S.Y., Abdullah, L.C., Siajam, S.I. and Yip, M.W., 2019. Utilization of Malaysia EAF slags for effective application in direct aqueous sequestration of carbon dioxide under ambient temperature. *Heliyon*, [e-journal] 5(10), p.e02602. https://doi.org/10.1016/j.heliyon.2019.e02602.

Pan, S.-Y., Chang, E.E. and Chiang, P.-C., 2012. CO2 Capture by Accelerated Carbonation of Alkaline Wastes: A Review on Its Principles and Applications. *Aerosol and Air Quality Research*, [e-journal] 12(5), pp.770–791. https://doi.org/10.4209/aaqr.2012.06.0149.

Pan, S.-Y., Chen, Y.-H., Fan, L.-S., Kim, H., Gao, X., Ling, T.-C., Chiang, P.-C., Pei, S.-L. and Gu, G., 2020. CO2 mineralization and utilization by alkaline solid wastes for potential carbon reduction. *Nature Sustainability*, [e-journal] 3(5), pp.399–405. https://doi.org/10.1038/s41893-020-0486-9.

Rahmanihanzaki, M. and Hemmati, A., 2022. A review of mineral carbonation by alkaline solidwaste. *International Journal of Greenhouse Gas Control*, [e-journal] 121(103798), pp.103798–103798. https://doi.org/10.1016/j.ijggc.2022.103798.

Ren, Z. and Li, D., 2023. Application of Steel Slag as an Aggregate in Concrete Production: A Review. *Materials*, [e-journal] 16(17), pp.5841–5841. https://doi.org/10.3390/ma16175841.

Romanov, V., Soong, Y., Carney, C., Rush, G.E., Nielsen, B. and O'Connor, W., 2015. Mineralization of Carbon Dioxide: A Literature Review. *ChemBioEng Reviews*, [e-journal] 2(4), pp.231–256. https://doi.org/10.1002/cben.201500002.

Rojas, N., Bustamante, M., Muñoz, P., Godoy, K. and Letelier, V., 2023. Study of properties and behavior of concrete containing EAF slag as coarse aggregate. *Developments in the Built Environment*, [e-journal] 14, pp.100137–100137. https://doi.org/10.1016/j.dibe.2023.100137.

Saadatkhah, N., Carillo Garcia, A., Ackermann, S., Leclerc, P., Latifi, M., Samih, S., Patience, G.S. and Chaouki, J., 2019. Experimental methods in chemical engineering: Thermogravimetric analysis—TGA. *The Canadian Journal of Chemical Engineering*, [e-journal] 98(1), pp.34–43. https://doi.org/10.1002/cjce.23673.

Sangita Meshram, Raut, S., Ansari, K., Madurwar, M.V., Md Daniyal, Mohammad Amir Khan, Katare, V.D., Afzal Husain Khan, Nadeem Ahmad Khan and Mohd Abul Hasan., 2023. Waste slags as sustainable construction materials: a compressive review on physico mechanical properties. *Journal of materials research and technology*, [e-journal] 23, pp.5821–5845. https://doi.org/10.1016/j.jmrt.2023.02.176.

Sanna, A., Uibu, M., Caramanna, G., Kuusik, R. and M. Maroto-Valer, M., 2014. A review of mineral carbonation technologies to sequester CO 2. *Chemical Society Reviews*, [e-journal] 43(23), pp.8049–8080. https://doi.org/10.1039/C4CS00035H.

Scimeca, M., Bischetti, S., Lamsira, H.K., Bonfiglio, R. and Bonanno, E., 2018. Energy Dispersive X-ray (EDX) microanalysis: A powerful tool in biomedical research and diagnosis. *European Journal of Histochemistry*, [e-journal] 62(1). https://doi.org/10.4081/ejh.2018.2841.

Singh, R., 2016. Production of Steel. *Applied Welding Engineering*, [e-journal] pp.37-55. https://doi.org/10.1016/b978-0-12-804176-5.00005-0.

Universiti Tunku Abdul Rahman., 2018. *X-ray Diffractometer*. [online image] *Universiti Tunku Abdul Rahman*. Available at: https://www2.utar.edu.my/fs/index.jsp?fcatid=194&fcontentid=843&f2ndcontentid=9502 [Accessed 2 Sep. 2023].

Ural, N., 2021. The significance of scanning electron microscopy (SEM) analysis on the microstructure of improved clay: An overview. *Open Geosciences*, [e-journal] 13(1), pp.197–218. https://doi.org/10.1515/geo-2020-0145.

Yildirim, I.Z. and Prezzi, M., 2011. Chemical, Mineralogical, and Morphological Properties of Steel Slag. *Advances in Civil Engineering*, [e-journal] 2011, pp.1–13. https://doi.org/10.1155/2011/463638.

Yu, J. and Wang, K., 2011. Study on Characteristics of Steel Slag for CO2Capture. *Energy & Fuels*, [e-journal] 25(11), pp.5483–5492. https://doi.org/10.1021/ef2004255.
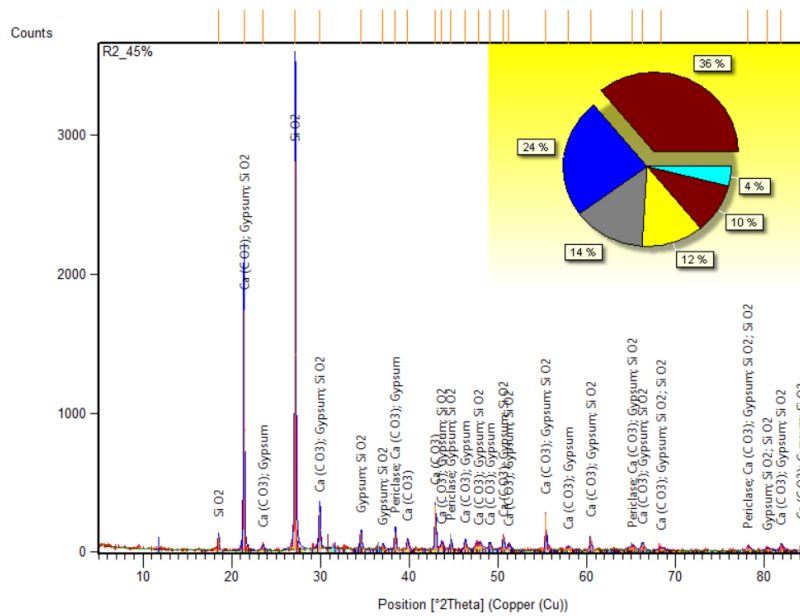
Zhang, Y., Yu, L., Cui, K., Wang, H. and Fu, T., 2023. Carbon capture and storage technology by steel-making slags: Recent progress and future challenges. *Chemical Engineering Journal*, [e-journal] 455, pp.140552–140552. https://doi.org/10.1016/j.cej.2022.140552.

APPENDICES

Appendix A: Graphs
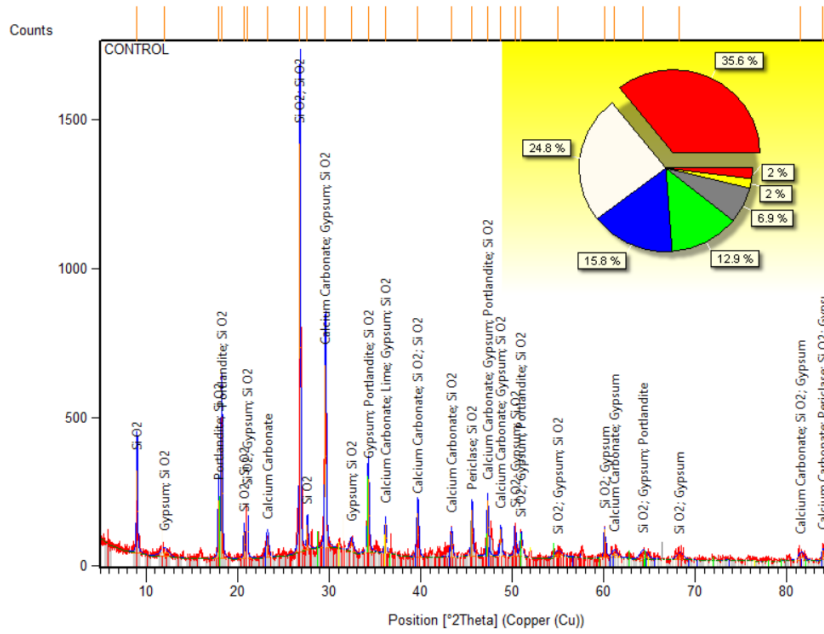
GraphA-1: XRD Graph of Control Set.

GraphA-2: XRD Graph of R2 45 %.

Appendix B: Tables

Density					
steel slag	=	2135	kg/m3		
sand	=	2650	kg/m3		
cement	=	3150	kg/m3		
Target Weigh	=	10.125	kg		
control	0%				
Cement	Sand	Water			
1	1	0.55		2.55	
		1 cube		3 cube	
Cement	=	3.97058824	kg	11.9117647	kg
Sand	=	3.97058824	kg	11.9117647	kg
Water	=	2.18382353	kg	6.55147059	kg

TableB-1:   Mix Proportion of Control Set Concrete.

Density						
steel slag	=	2135	kg/m3			
sand	=	1520	kg/m3			
cement	=	3150	kg/m3			
Target Weigh	=	10.125	kg			
Replacement	15%	0.15				
	Cement	Sand	Slag	water		
	1.000	0.850	0.211	0.550		2.611
		1 cube		3 cube		9 cube
Cement	=	3.878	kg	11.635	kg	34.905
Sand	=	3.297	kg	9.890	kg	29.669
Steel Slag	=	0.817	kg	2.451	kg	7.354
Water	=	2.133	kg	6.399	kg	19.198

TableB-2:   Mix Proportion of R1 15 % EAF Slag Concrete.

Range 1 (R1) :	2.36mm-0.8mm		Cube Dimension :	150mmx150mmx150mm	
Range 2 (R2) :	4.75mm-2.36mm				
Range 3 (R3) :	7 mm-4.75mm				
Control	Fresh Mass	Fresh Density	Hardened Mass	Hardened Density	Compressive Strength
	(kg)	(kg/m^3)	(kg)	(kg/m^3)	(kN)
Cube 1	6.91	2,048.62	7.02	2,079.41	537.90
Cube 2	6.90	2,045.84	7.01	2,077.19	611.50
Cube 3	6.94	2,057.63	7.05	2,087.41	524.00
	6.92	2,050.70	7.02	2,081.33	557.80
R1 (15%)	Fresh Mass	Fresh Density	Hardened Mass	Hardened Density	Compressive Strength
	(kg)	(kg/m^3)	(kg)	(kg/m^3)	(kN)
Cube 1	7.04	2,085.48	7.18	2,126.81	439.30
Cube 2	6.93	2,054.77	7.04	2,085.63	441.00
Cube 3	7.13	2,111.27	7.25	2,147.11	457.10
	7.03	2,083.84	7.15	2,119.85	445.80
R1 (30%)	Fresh Mass	Fresh Density	Hardened Mass	Hardened Density	Compressive Strength
	(kg)	(kg/m^3)	(kg)	(kg/m^3)	(kN)
Cube 1	7.45	2,206.81	7.54	2,233.48	790.80
Cube 2	7.46	2,209.63	7.55	2,237.63	627.70
Cube 3	7.47	2,214.07	7.57	2,242.22	575.40
	7.46	2,210.17	7.55	2,237.78	664.63
R1 (45%)	Fresh Mass	Fresh Density	Hardened Mass	Hardened Density	Compressive Strength
	(kg)	(kg/m^3)	(kg)	(kg/m^3)	(kN)
Cube 1	7.66	2,268.44	7.76	2,298.67	789.80
Cube 2	7.67	2,272.89	7.77	2,302.96	841.40
Cube 3	7.68	2,275.41	7.78	2,303.85	572.00
	7.67	2,272.25	7.77	2,301.83	734.40

TableB-3: Compressive Strength Result of Control and R1 Group EAF Slag Concrete.

R2 (15%)	Fresh Mass	Fresh Density	Hardened Mass	Hardened Density	Compressive Strength
	(kg)	(kg/m^3)	(kg)	(kg/m^3)	(kN)
Cube 1	7.56	2,238.96	7.64	2,264.15	586.00
Cube 2	7.48	2,217.33	7.57	2,243.70	557.80
Cube 3	7.33	2,172.74	7.43	2,201.48	565.80
0.00	7.46	2,209.68	7.55	2,236.44	569.87

R2 (30%)	Fresh Mass	Fresh Density	Hardened Mass	Hardened Density	Compressive Strength
	(kg)	(kg/m^3)	(kg)	(kg/m^3)	(kN)
Cube 1	7.54	2,235.26	7.64	2,264.15	848.30
Cube 2	7.57	2,241.78	7.66	2,268.15	780.90
Cube 3	7.54	2,233.63	7.61	2,255.41	706.80
0.00	7.55	2,236.89	7.64	2,262.57	778.67

R2 (45%)	Fresh Mass	Fresh Density	Hardened Mass	Hardened Density	Compressive Strength
	(kg)	(kg/m^3)	(kg)	(kg/m^3)	(kN)
Cube 1	7.73	2,289.19	7.81	2,313.04	823.10
Cube 2	7.73	2,289.78	7.84	2,322.67	827.40
Cube 3	7.71	2,284.00	7.81	2,315.41	832.70
0.00	7.72	2,287.65	7.82	2,317.04	827.73

R3 (15%)	Fresh Mass	Fresh Density	Hardened Mass	Hardened Density	Compressive Strength
	(kg)	(kg/m^3)	(kg)	(kg/m^3)	(kN)
Cube 1	7.41	2,196.30	7.52	2,229.19	692.10
Cube 2	7.40	2,191.85	7.52	2,228.30	671.20
Cube 3	7.40	2,193.48	7.50	2,222.37	690.20
0.00	7.40	2,193.88	7.51	2,226.62	684.50

R3 (30%)	Fresh Mass	Fresh Density	Hardened Mass	Hardened Density	Compressive Strength
	(kg)	(kg/m^3)	(kg)	(kg/m^3)	(kN)
Cube 1	7.60	2,252.15	7.70	2,282.07	842.50
Cube 2	7.61	2,253.93	7.71	2,283.11	872.10
Cube 3	7.59	2,249.04	7.70	2,280.59	814.20
0.00	7.60	2,251.70	7.70	2,281.93	842.93

R3 (45%)	Fresh Mass	Fresh Density	Hardened Mass	Hardened Density	Compressive Strength
	(kg)	(kg/m^3)	(kg)	(kg/m^3)	(kN)
Cube 1	7.79	2,308.89	7.89	2,337.93	902.90
Cube 2	7.74	2,293.93	7.80	2,310.81	770.20
Cube 3	7.91	2,343.85	7.99	2,367.85	966.60
0.00	7.82	2,315.56	7.89	2,338.86	879.90

TableB-4:   Compressive Strength Result of R2 and R3 Group EAF Slag
Concrete.